scientific reports

OPEN

Design storm estimation for flood risk assessment in the temperate Himalayan basin using hydrological modelling

Mohmmad Idrees Attar[1✉], Junaid Nazir Khan[1], Yasir Altaf[2✉], Majed Alsubih[5], Sameena Naseer[1], Rohitashw Kumar[1], Owais Ahmad Bhat[1], Shabir Ahmad Bangroo[3] & M. K. Sharma[4]

Flood frequency analysis and hydrological modelling are crucial for water resource management and flood mitigation, especially in regions vulnerable to extreme weather. This study utilises the HEC-HMS hydrological model to simulate rainfall-runoff processes and generate design storms for various return periods across 24 sub-watersheds of the Jhelum Basin, Kashmir. The model setup includes rainfall transformation using the ModClark method, baseflow estimation through the Linear Reservoir Method, and flood routing via the Muskingum approach. Satellite-based gridded rainfall data and sub-basin-specific hyetographs were used as meteorological inputs to ensure spatially distributed precipitation representation. Calibration and validation were performed using discharge data from Sangam, Ram Munshibagh, and Asham gauging stations (2020–2023), covering five high-flow events. This research marks the first application of event-based design storms at the sub-watershed scale in the Kashmir Valley using HEC-HMS, providing high-resolution insights into flood risk patterns. The model showed strong agreement with observed hydrographs ($R^2 > 0.78$, NSE > 0.56, RSR < 0.6, PBIAS within ± 25%). Sensitivity analysis identified curve number, time of concentration, and infiltration rates as key parameters influencing performance. Results indicated varied hydrological responses, with watersheds like Lower Jhelum, Sindh, Lidder, and Pohru showing higher peak discharges due to steep slopes, while low-lying areas such as Wular-II and Anchar exhibited prolonged flood retention. Urbanised watersheds like Dal and Wular-I showed moderate to high peaks, highlighting infrastructure vulnerability. Design storms for 2–500-year return periods identified critical flood-prone zones, offering insights for infrastructure planning and risk management. This research highlights the effectiveness of HEC-HMS model as an important non-structural flood mitigation measure in a mountainous region of Kashmir.

Keywords Design storm, Flood, HEC-HMS, Hydrological modelling, Jhelum basin

Hydrological modelling is an important tool in water resource planning, flood hazard mapping and infrastructure design[1–3]. It simulated the hydrological processes such as precipitation, infiltration, surface runoff, and channel flow to predict how the water will flow in a watershed[4–6]. Hydrologic Engineering Center's Hydrologic Modelling System (HEC-HMS) is the most commonly used model among the commonly used hydrological models to analyse flood risks under different hydrological conditions[7–9]. The integration of these models with remote sensing (RS) and geographic information system (GIS) technologies has significantly increased the accuracy of these models[10].

Event-based rainfall-runoff models simulate the hydrologic responses of individual peak storm events, which makes them ideal for flood forecasting and infrastructure design[11,12]. These models differ from continuous models in the aspect that they focus on individual storms, hence eliminating the computational needs but capturing peak discharges, which are needed for infrastructure design[9]. The models prove useful in

[1]College of Agricultural Engineering and Technology, SKUAST-Kashmir, Shalimar Srinagar 190025, India. [2]Department of Environmental Sustainability and Climate Change, IUST, Awantipora 192122, India. [3]Division of Soil Science, FOH, SKUAST-Kashmir, Shalimar Srinagar 190025, India. [4]Division of Fruit Science, FOH, SKUAST-Kashmir, Shalimar Srinagar 190025, India. [5]Civil Engineering Department, College of Engineering, King Khalid University, Abha 61421, Saudi Arabia. ✉email: attaridrees@gmail.com; yasiraltaf1988@gmail.com

areas with poor data availability, as in the Kashmir region, where flash flood occurrence and variable rainfalls necessitate efficient stormwater management strategies[13]. Loss (infiltration), transformation (generation of runoff), and routing processes form the essential elements, each of which is to be calibrated based according to local conditions[7,14,15]. HEC-HMS is broadly used for event-based modelling. Its modular structure supports various methods: SCS Curve Number for losses, Snyder's Unit Hydrograph for transformation, and Muskingum routing[16]. Many studies globally have employed hydrological models to analyse flood dynamics and develop design storms. HEC-HMS was introduced by the U.S. Army Corps of Engineers (USACE) as a successor to HEC-1, with capabilities of advanced hydrological simulation[16–18]. The efficiency of HEC-HMS in the assessment of flood peaks and hydrographs at different return periods has been reported by several studies. Early studies[19–21] showed the reliability of the HEC-HMS model in simulating rainfall runoff processes. Furthermore, some studies showed the effect of climate change[22] and land-use change analysis[23] on flood vulnerability, which highlights a rising susceptibility to flood risks. Recent studies have included radar-based rainfall integration for urban floods[24] coupled with HEC-HMS/HEC-RAS modelling for hazard mapping[25] and transboundary flood assessments[26]. These studies highlight the effectiveness of HEC-HMS for flood risk management under different geographical and hydrological conditions.

In India, HEC-HMS has been widely used for flood simulations of major river basins. Mandal and Chakrabarty[27] used HEC-HMS coupled with HEC-RAS to showcase the utility of the model in mountainous basins by simulating flash floods in the Teesta Watershed and delineating flood-prone areas. Koneti et al.[28] estimated the effect of land use changes on runoff processes and found the model to be reliable for long-term hydrological modelling. In urban flood studies, Rangari et al.[29] applied HEC-HMS to simulate extreme storm events in Hyderabad, identifying drainage limitations with a peak discharge of 590.5 m³/s. Natarajan and Radhakrishnan[17] further focused on the need for an integrated hydrologic and hydraulic modelling approach in urban flood studies. Dimri et al.[30] modelled streamflows for the Tehri Dam reservoir, showing the capability of the model in capturing seasonal variability. Vegad et al.[31] highlighted the role of reservoir operations in flood management by simulating the historical floods of the Ganga-Brahmputra catchments.

Numerous comparative studies have underscored the strengths of HEC-HMS over alternative models such as SWAT, MIKE NAM, HBV, and artificial neural networks (ANN), especially for event-based flood modelling. In a recent study in the sub-humid tropical Kabini Basin of Kerala, Prakash et al.[32] demonstrated that HEC-HMS outperformed SWAT in simulating peak discharges, making it more suitable for flood-focused hydrological modelling in Indian conditions. Similarly, Tibangayuka et al.[33] evaluated HEC-HMS, HBV, and ANN models in a high-humidity, data-scarce tropical catchment and found HEC-HMS to be superior, achieving NSE values of 0.84 during validation, compared to 0.64 for HBV and 0.55 for ANN. These results underscore the robustness of HEC-HMS in replicating observed hydrographs under variable data availability and climatic regimes. Vo et al.[34] compared MIKE NAM, MIKE SHE, SWAT, and HEC-HMS in two Vietnamese stations. Their findings showed that HEC-HMS and MIKE SHE consistently achieved high correlation coefficients and lower RMSE values during both calibration and validation, outperforming both MIKE NAM and SWAT. Recent studies suggest that coupling HEC-HMS with machine learning enhances simulation accuracy in data-scarce catchments. Mugume et al.[35] and Narayana Reddy and Pramada[36] demonstrated the effectiveness of HEC-HMS–ANN hybrids for improved streamflow and runoff predictions, indicating a promising direction for future hydrologic modelling.

Advances in hybrid methods now couple hydrodynamic models with machine learning techniques, improving the flood hazard susceptibility mapping in a mountainous–urban environment[37]. Sensitivity analysis of 2D flood inundation models, such as the Tous Dam study, has highlighted the importance of model parameters in simulating flood extent[38]. Risk based design tools built on hydrodynamic simulations can visualise how flood protection dikes redistribute expected annual damages across a floodplain[39]. In a similar context, Tariq et al[40]. emphasises on selecting measures that align with risk based flood management principles rather than fixed return period practices. Hanif et al[41]. demonstrated that high-resolution satellite-derived land cover classifications, generated using machine learning algorithms, have a significant impact on hydrological model outputs, thereby underscoring the necessity of incorporating fine-scale inputs for accurate simulation and analysis. In this context, this study is novel in its event-based, sub-watershed-scale simulation using high-resolution rainfall inputs to derive design storms for multiple return periods across 24 sub-watersheds in the Jhelum Basin, an aspect that remains underexplored in the literature.

Lately, the urban centres such as Srinagar, Anantnag and Baramulla of Kashmir Valley have been experiencing uncontrolled urbanisation[42,43]. This unplanned urbanisation, along with changing land-use patterns[44] and increasing climate variability, has significantly amplified the susceptibility of the Jhelum river and its tributaries to disastrous flood events[45,46]. The past floods, especially the 2014 flood, highlight the growing flood risk in the region[47,48]. Previous studies[49–53] have employed various hydrological and hydraulic models—including MIKE 11 NAM, SWAT, HEC-RAS, and HEC-HMS to examine flood behaviour in the valley. However, most of these studies have focused on long-term hydrological trends or large-scale analyses, often overlooking short-duration, event-based flood simulations at the sub-watershed level.

Despite existing studies on flood modelling in the Kashmir Valley, there is a lack of comprehensive research on design storm development and event-based hydrological analysis for sub-watersheds. The IDF curve study by Dar and Maqbool[54] was limited to data from only six rainfall gauging stations, which constrains its spatial representativeness and leaves many smaller sub-watersheds in the Kashmir Valley inadequately characterised in terms of flood risk. However, flood response is highly sensitive to spatial heterogeneity in terrain, soil types, and land use patterns, factors that vary considerably across the valley. Addressing this variability requires a high-resolution rainfall and finer modelling scale that can reveal localised flood characteristics and inform site-specific risk management.

The core objective of this study is to generate sub-watershed level design storms in the data-scarce Jhelum Basin using an event-based HEC-HMS framework. This is achieved by integrating high-resolution, gridded

satellite rainfall data to construct hyetographs for varying return periods and applying them across 24 delineated sub-watersheds. By focusing on sub-watershed scale analysis, this study captures the spatial variability in flood behaviour driven by topography, land use, and soil conditions, offering a more precise understanding of flood risks and hydrologic responses.

This research fills a critical gap by demonstrating how high-resolution rainfall inputs and distributed event-based modelling can be applied effectively in data-limited mountainous basins. The findings aim to support improved flood forecasting, localised hazard mapping, and adaptive flood management strategies for the Kashmir Valley.

Materials and methods
Study area
This study focuses on the Jhelum River Basin within the Kashmir Valley, extending up to its watershed outlet at Uri, a crucial hydrological unit of the larger Jhelum River system, which lies within the northwestern Himalayas. The basin is located geographically between the latitudes 33°20′30″N and 34°40′40″N and longitudes 73°42′30″E and 75°45′23″E, covering an area of 13,530.8 km[2]. The valley consists of alluvial plains in the low-lying areas and Himalayan peaks surrounding these plains, with elevation ranging from 1,069 m to 5,361 m above sea level, leading to different climatic and hydrological conditions. The basin encompasses 24 major watersheds (Fig. 1), each possessing unique hydro-geomorphological characteristics that control water movement in the basin[55]. The main soil types in the region include loamy and clay loam textures, which control the groundwater recharge and storage[56] (Fig. 2) (Fig. S1 of the supplementary appendix). The valley is dominated by forest and horticulture land uses (Fig. S2 of the supplementary appendix). The annual temperature in the region varies from a low of −10 °C during winter to a high of 35 °C in summer[57,58]. The region receives precipitation both in the form of rainfall and snow[59] with a mean annual rainfall of approximately 840 mm[60] and an average snowfall depth of around 30–35 cm, which has shown a declining trend over recent decades[61].

Data sets used
The study employed multiple datasets, as listed in Table 1 for model development, calibration, and validation.
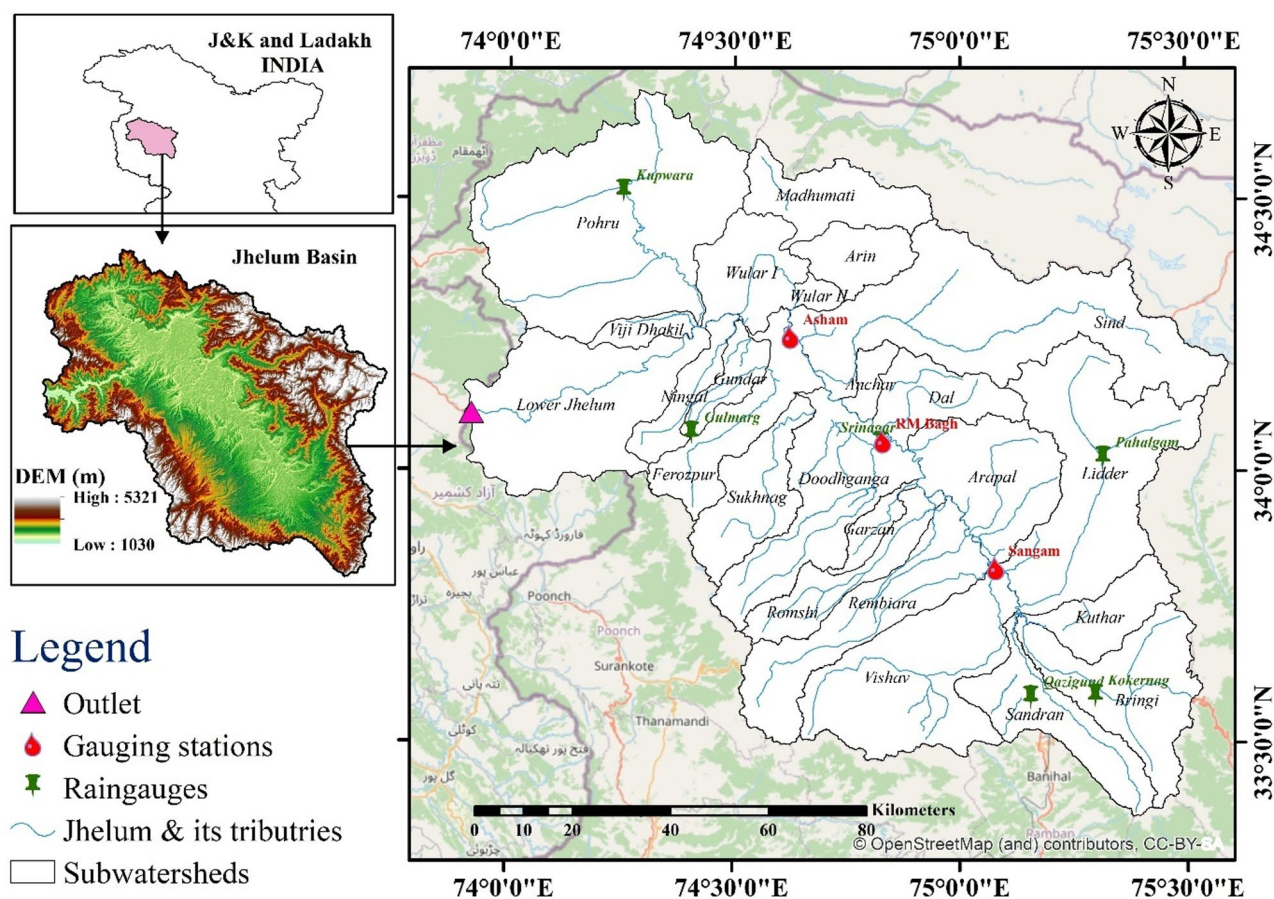

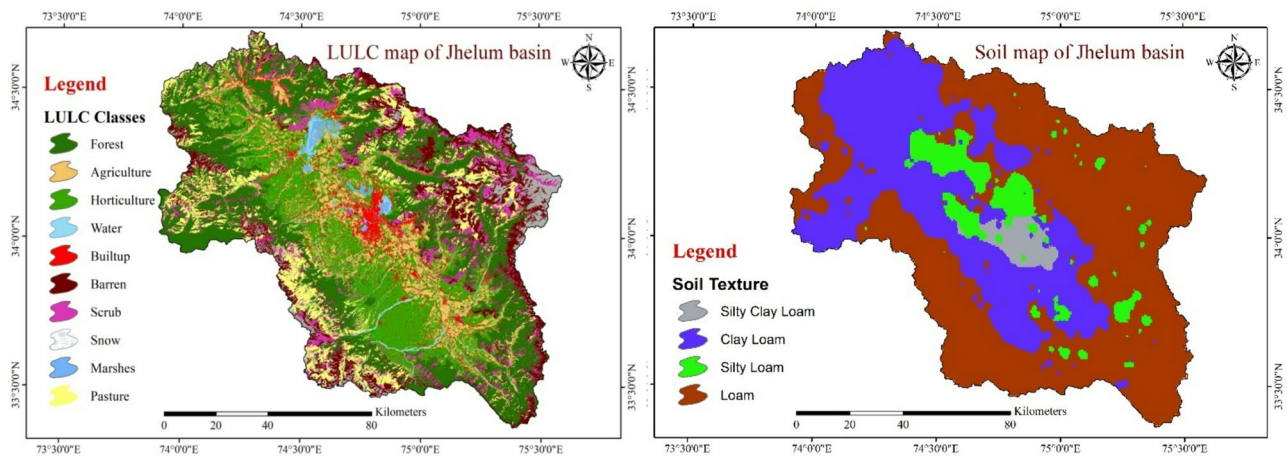**Fig. 1.** Geographic and Topographic map of study area.(Source: SRTM DEM, https://earthexplorer.usgs.gov).

Fig. 2. LULC and Soil maps of Jhelum basin.(Source: generated from data obtained from https://earthexplorer.usgs.gov/).

Data Type	Source	Application
DEM	SRTM (30 m resolution), USGS Earth Explorer	Basin delineation, watershed extraction
Soil map	Prepared in SAGA GIS using soil texture data	CN Grid generation
LULC Map	Prepared used supervised classification of the Landsat 8 image (USGS Earth Explorer)	
Satellite-based Gridded Rainfall Data	CHIRPS, (4.8 × 4.8 km resolution, 1980–2023, ClimateEngine.org)	Hyetograph and Design storm generation for 24 watersheds
Gridded Rainfall Data	IMD (India Meteorological Department), 25*25 km, resolution	Generation of Simulated flows at Sangam, Ram Munshibagh, Asham for model calibration and validation
Daily Discharge Data	Irrigation & Flood Control Department, Kashmir	Model calibration and validation at Sangam, Ram Munshibagh, Asham

Table 1. Summary of data sources and applications for hydrological Modelling.

Methodology

The Jhelum Basin and its subwatersheds were delineated using a 30 m spatial resolution SRTM DEM in HECGeo-HMS. The land use/land cover (LULC) (Fig. 2) and the soil maps were processed in ArcMap 10.8 to derive a hydrological soil group map (HSG) and Curve Number (CN) grid (Fig. S3 and Fig. S4 of the supplementary appendix) for the study area, which was subsequently incorporated into the parameters file of the HEC-HMS model to simulate rainfall-runoff processes at the subbasin level. Spatially distributed rainfall inputs were derived from two sources: long-term Climate Hazards Group InfraRed Precipitation with Station data (CHIRPS) gridded rainfall data (1980–2022), (Fig. S5 of supplementary appendix), used to develop watershed-specific hyetographs and design storms, and IMD gridded rainfall DSS (Data Storage System) data (August 2020–August 2023), employed to calibrate the generated runoff hydrographs. Calibration of the model was performed with daily streamflow records at Sangam, Ram Munshibagh, and Asham gauging stations. Finally, design storms for varying return periods were simulated in the model to calculate peak discharges across the 24 sub-watersheds. The methodological workflow is summarised in Fig. 3.

Model development

The basic structure of the model comprises a (i) Basin model, (ii) Meteorological model, (iii) Control specification, and (iv) Time series manager. The hydrological model of the Jhelum basin, developed using the HEC-HMS program, is shown in Fig. 4.

Development of basin model

The basin model of grid resolution of 2 km x 2 km was developed using terrain pre-processing and basin processing in HEC-GeoHMS. Terrain pre-processing involves a series of steps for generating the stream network, basin boundary, and drainage outlets[62,63]. The outlet is defined by a batch point, and then the upstream watershed is discretised into sub-basins[64]. Creating a basin model of the Jhelum basin for adding various watershed characteristics and parameters into the model is the first step towards model development. To complete this step, a control point was set up at the outlet of the lower Jhelum subbasin[51].
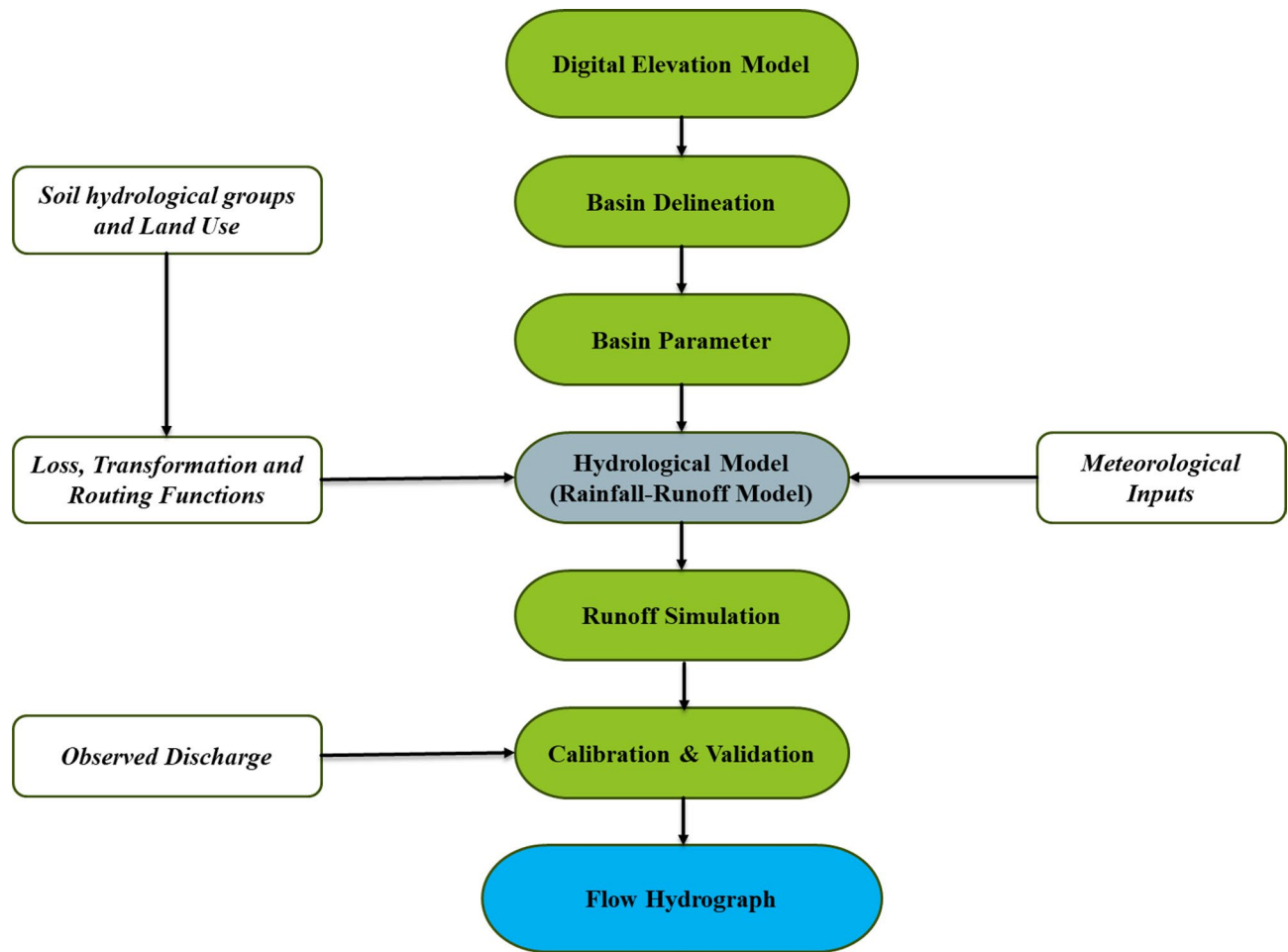
Fig. 3. Methodology Framework.

Estimation of initial losses
The Soil Conservation Service Curve Number (SCS-CN) method[65] was used to calculate the initial losses (Eq. 1), due to its suitability for event-based rainfall-runoff modelling and minimal input requirements, which was helpful in the data-scarce Jhelum Basin[66,67]. A spatially distributed CN grid was used to estimate the infiltration losses across sub-basins.

$$Q = \frac{(P - I_a)^2}{(P - I_a - S)}; \ I_a = 02\ S; \ Q = \frac{(P - 0.2S)^2}{(P + 0.8S)}; \ S = \frac{25400}{CN} - 254 \tag{1}$$

Where, Q = direct runoff; P = precipitation; I_a = Initial abstraction; S = potential maximum retention; CN = Curve Number.

Transformation of rainfall to runoff
The ModClark transformation method[68] was utilised to convert rainfall into runoff. The ModClark method was selected over the Snyder unit hydrograph because it is explicitly designed for gridded precipitation inputs[16]. This method combines a gridded time-area histogram with linear reservoir routing, improving spatial representation compared to the lumped time-area approach in the original Clark method[16,69]. The watershed is discretised into grid cells, each assigned a travel time index ($T_{t,\ cell}$) relative to the watershed's time of concentration ($T_{c,\ watershed}$) and its normalised flow distance:

$$T_{t,cell} = T_{c,watershed}\left(D_{cell}/D_{\max}\right) \tag{2}$$

Where, D_{cell} = distance from a specific grid cell to the outlet of the basin; D_{max} = Longest travel path from grid cell to outlet.

The primary input parameters include T_c and storage coefficient, both of which were derived using basin geomorphological parameters such as watershed area, longest flow path, and basin slope. The T_c was calculated using the using the Kirpich empirical formula proposed by Kirpich[70] as shown in Eq. (3).
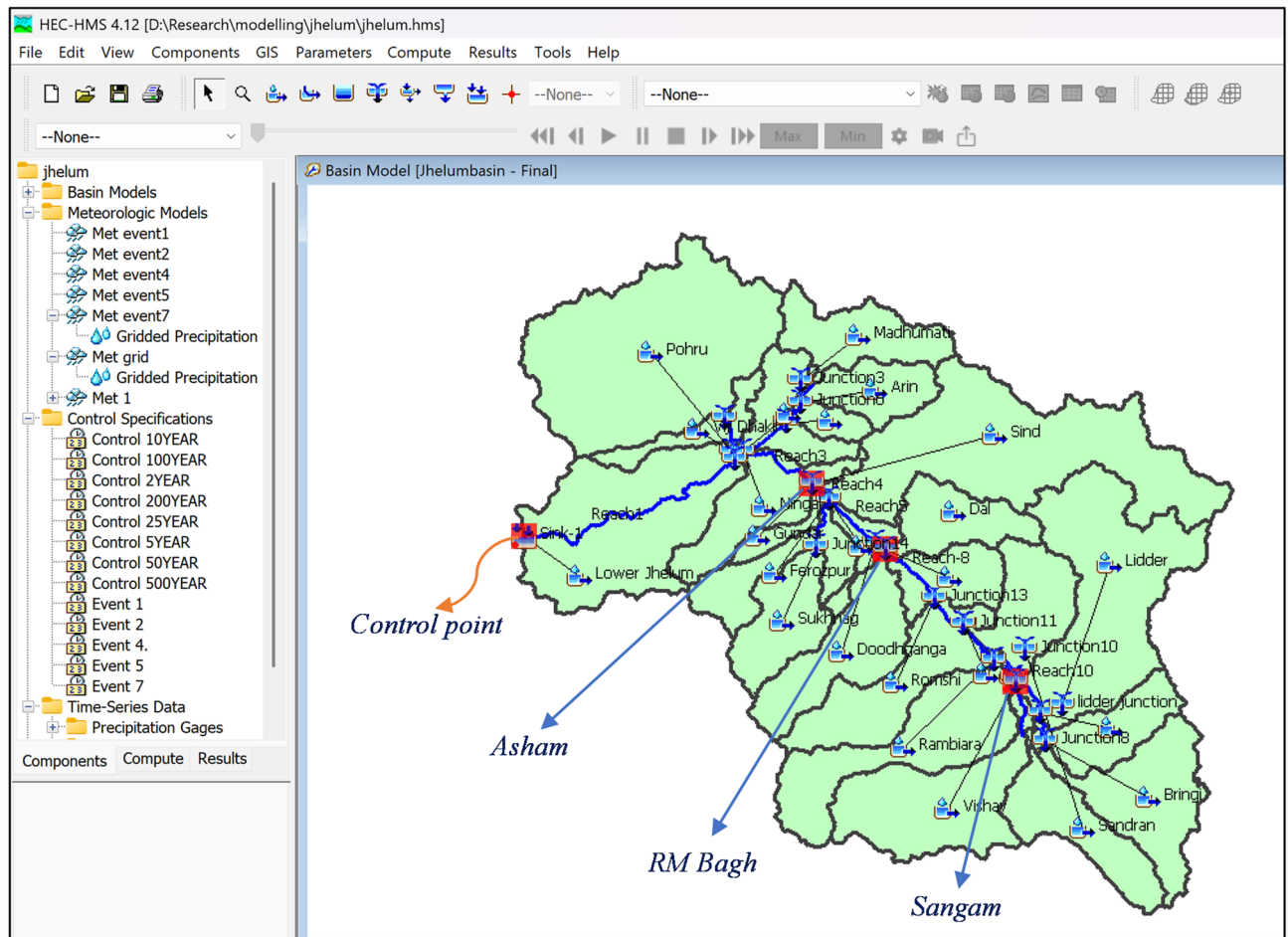
Fig. 4. Basin model of the Jhelum basin.(Source: generated in HEC-HMS 4.12 software using data obtained from https://earthexplorer.usgs.gov/).

$$T_c = 0.0195 \frac{L^{0.77}}{S^{0.385}} \qquad (3)$$

Where, T_c = time of concentration; L = Basin length and S = basin slope.

Estimation of baseflow

The Linear Reservoir Method was utilised to simulate subsurface flow processes, effectively representing baseflow contributions to streamflow in event-based modelling applications[71,72]. This method employs one to three linear reservoirs (layers) to model baseflow recession following a storm event. In this study, two reservoirs were employed with initial conditions comprising a baseflow of 1 m³/s, a partition fraction of 0.5, and two routing steps per layer. The routing coefficient was set equal to the storage coefficient for each subbasin to ensure that the routing time interval aligned with the natural drainage rate of the storage element. This alignment preserves the physical behaviour of baseflow recession and minimises numerical damping. The trial-and-error method was used to optimise these parameters through calibration.

Channel routing setup

Flood wave propagation was modelled using the Muskingum routing method[73,74], which solves the continuity equation to calculate outflow (O_t) and storage while accounting for hysteresis effects. The Muskingum method was selected due to the limited availability of channel cross-sectional data for the Jhelum River and its demonstrated reliability in previous studies of ungauged basins[75]. The governing equation[76] (Eq. 4) is expressed as:

$$O_t = \left(\frac{\Delta t - 2KX}{2K(1-X) + \Delta t} \right) I_t + \left(\frac{\Delta t - 2KX}{2K(1-X) + \Delta t} \right) I_{t-1} + \left(\frac{2K(1-X) - \Delta t}{2K(1-X) + \Delta t} \right) O_{t-1} \qquad (4)$$

where O_t and I_t are the outflow (m³/s) and inflow (m³/s) at time t, respectively; K is the travel time of the flood wave (hours); X is a dimensionless weighting factor ($0 \le X \le 0.5$); and Δt is the computational time step (hours).

In this study, the value weighing factor (X) was assigned as 0.2, and the time of travel (K) for all 11 delineated reaches was calculated using Kirpich's formula (Eq. 3).

A constant loss/gain method was used to simulate bidirectional interactions between streamflow and subsurface storage, capturing both losses (such as infiltration from the channel into groundwater) and gains (such as baseflow contributions from groundwater to the stream). This method was selected due to its minimal data requirements and compatibility with all routing techniques available in HEC-HMS[16]. It operates by applying a constant volumetric rate and a fractional adjustment to the routed flow at each reach, thus approximating stream–aquifer exchanges. In the absence of spatially distributed groundwater data, this approach offers a simplified yet effective means to represent subsurface flow processes. The loss/gain parameters were applied uniformly across all delineated reaches. The meteorological model defines the boundary conditions for the watershed throughout the simulation period and governs the spatial and temporal distribution of rainfall throughout individual sub-basins[77,78]. In this study, two metrological models were developed, one by using IMD gridded rainfall as a precipitation method and the other by specified hyetographs for each subbasin.

The control specification is a crucial aspect of the project that manages simulation runs, defining their start and end times. Five control specifications were set up for five identified peak events and eight additional ones for eight different return periods. The time series data manager assigns daily records of precipitation and streamflow, with computations conducted on a daily time step. In order to assign the required data, twenty-four (24) precipitation gauges for 24 subbasins and three (3) discharge gauges for three (3) computation points, namely Sangam, Ram Munshibagh and Asham, were set up. In addition to the above, a gridded data manager was set up to add IMD's gridded rainfall DSS for the watershed.

Calibration and validation

Calibration systematically fine-tunes watershed parameters to ensure the simulated hydrograph closely aligns with the observed hydrograph[79,80]. In this study, the HEC-HMS model was calibrated and validated using daily discharge data from three gauging stations—Sangam, Ram Munshibagh, and Asham—spanning August 2020 to August 2023. Five significant flood peak events were identified during this period. The first three events (2020–2021) were utilised for calibration, while the last two (2022–2023) were used for validation. A manual calibration was used, where the initial parameter estimates obtained during hydrologic pre-processing were iteratively adjusted through a trial-and-error approach to assess optimal model parameters. Model performance was assessed using the coefficient of determination (R^2), Nash-Sutcliffe Efficiency (NSE), RMSE-observations standard deviation ratio (RSR) and percent bias (PBIAS)[81–84]. The coefficient of determination (R^2) quantifies the strength of the linear relationship between observed and simulated values, with values ≥ 0.70 generally reflecting good model performance. The Nash–Sutcliffe Efficiency (NSE) assesses the predictive accuracy of the model, where values > 0.5 are deemed acceptable. The RMSE–standard deviation ratio (RSR), which normalizes the root mean square error by the standard deviation of observed data, is considered indicative of good performance when values are ≤ 0.60. Percent bias (PBIAS), which measures the average tendency of the simulated values to over- or underpredict observations, is regarded as satisfactory when the absolute value falls within $\pm 25\%$[16]. Sensitivity analysis was carried out alongside calibration to identify the critical watershed parameters. The calibrated model was then evaluated for its predictive capability and subsequently used to generate flood hydrographs (design storms) at the sub-basin level for various return periods.

Results and discussions
Sensitivity analysis

Sensitivity analysis aids in understanding the responsiveness of model outputs to input parameters and informs calibration priorities[85,86]. Given the event-based modelling approach and limited availability of high-resolution input data, the analysis focused on parameters associated with the SCS-CN loss method, ModClark transformation, linear reservoir baseflow, and Muskingum channel routing. Among the tested parameters, the Curve Number (CN) exhibited the highest sensitivity, with a $\pm 5\%$ variation causing up to 12% deviation in peak discharge and 9% in runoff volume, which is consistent with findings from earlier studies[87]. Time of concentration (T_c) and storage coefficient from the ModClark method significantly influenced hydrograph timing and attenuation. Adjustments to T_c altered the lag between rainfall and runoff response, while the storage coefficient modulated peak attenuation. This shows the importance of basin geomorphology in flood simulation and the effectiveness of Kirpich's empirical equation[70] for estimating T_c based on slope and flow length. In Muskingum routing, the travel time (K) impacted outflow peaks more than the weighting factor (X). Parameters related to baseflow (routing coefficient, partition fraction) showed moderate sensitivity, mainly affecting the hydrograph's recession limb. This insight was instrumental in guiding the manual calibration process, emphasising CN, T_c and K as the critical parameters and supporting prioritisation of these parameters in future studies and uncertainty assessments. Table 2 summarises the relative sensitivity of the key parameters.

Calibration and validation

The model was calibrated at three important gauging sites along the main Jhelum River using three observed events to ensure the model's reliability for simulating storm runoff in the Jhelum Basin (Table S1 of the supplementary appendix). During the calibration phase (Events 1–3), the model exhibited strong agreement with observed discharge (Figs. 5, 6 and 7), with R^2 ranging from 0.78 to 0.98, NSE values between 0.568 and 0.894 and RSR values of 0.3 to 0.6. PBIAS values largely fell within the acceptable range of $\pm 25\%$ (Table 3). The slightly higher negative biases during Event 2 at RM Bagh (−20.44%) and Asham (−17.98%) suggest localised overestimation. These deviations may be attributed to spatial variability in rainfall, antecedent soil moisture conditions, or limitations in capturing urbanised flow dynamics[88,89]. These results confirm the model's capability to simulate event-based runoff across spatially diverse catchments[88].

Parameter	Method	Sensitivity Type	Impact on Output	Rank
CN	SCS-CN	Loss	± 12% peak flow	1
T_c	ModClark	Routing	± 2 h peak shift	2
K	Muskingum	Routing	± 9% flow volume	3
Storage Coefficient	ModClark	Routing	Moderate hydrograph shape	4
Routing Coefficient	Linear Reservoir	Baseflow	Recession limb	5

Table 2. Summary of the relative sensitivity of the key parameters.
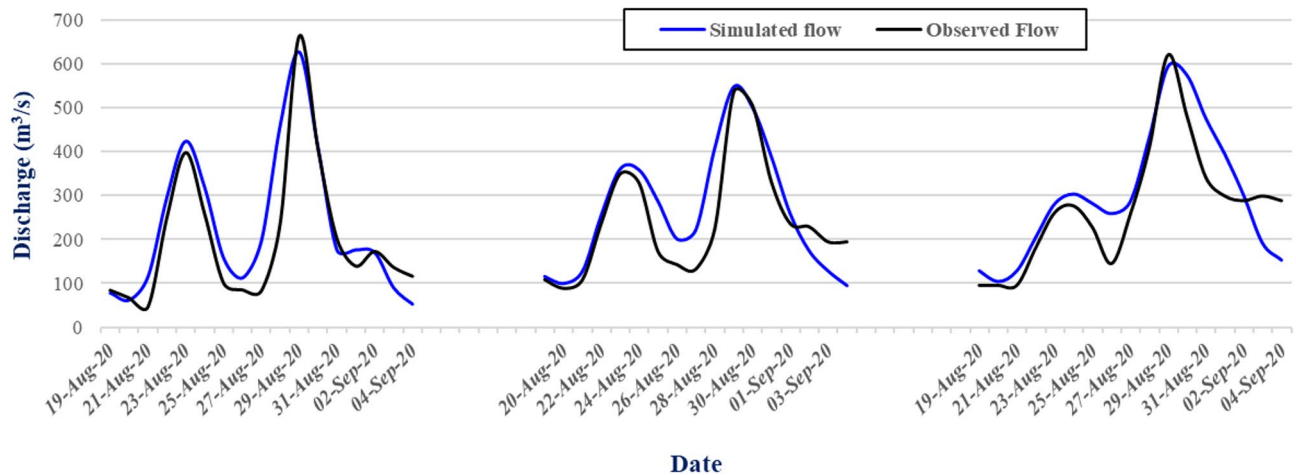
Fig. 5. Plot of Observed vs. Simulated flow at three stations for Event 1 (19-Aug-2020 to 04-Sep-2020).
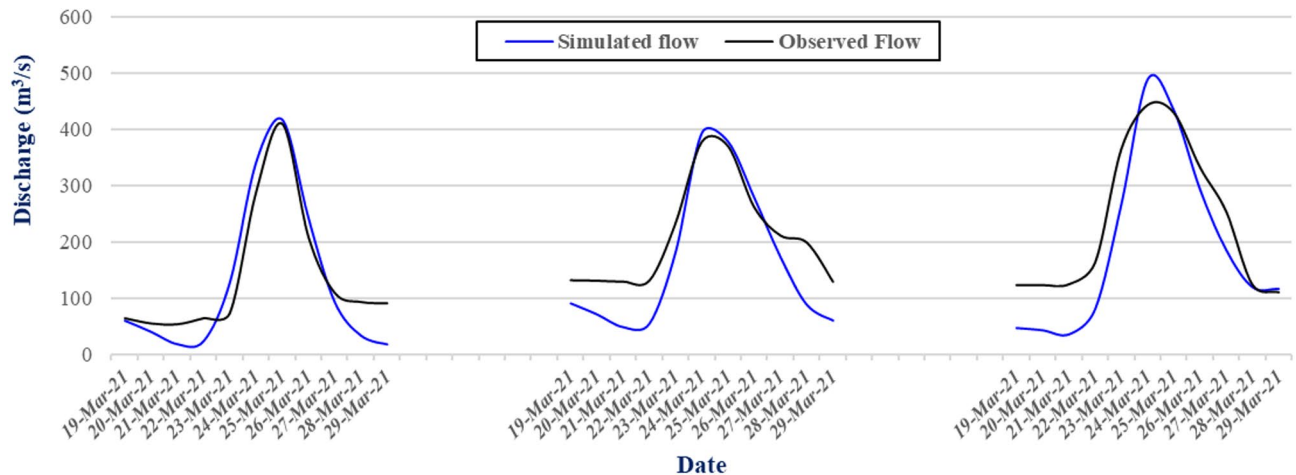
Fig. 6. Plot of Observed vs. simulated flow at three stations for Event 2 (19-Mar-21 to 29-Mar-21).

In the validation phase (Events 4–5) (Table S2 of the supplementary appendix), model performance remained consistent or improved, reinforcing the robustness of the calibrated parameters (Figs. 8 and 9). R² values exceeded 0.80 across all sites, reaching as high as 0.97 at RM Bagh in Event 5. NSE values also remained strong (≥ 0.70 at all locations), with the highest efficiency (0.92) observed at Sangam. Although PBIAS values were slightly negative during validation (ranging from − 17.68% to − 10.97% in most cases), they remained well within acceptable thresholds, indicating moderate overprediction but no systematic bias (Table 4).

The model's consistent performance in both calibration and validation phases, especially in achieving R² > 0.79, NSE > 0.56, RSR < 0.6 and |PBIAS| < 25% across varied events, underscores its suitability for flood risk
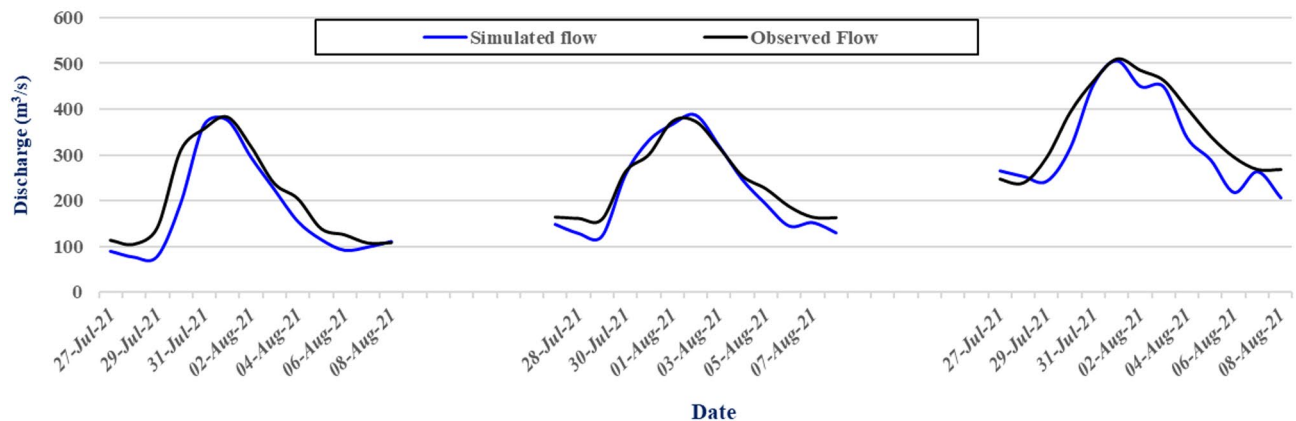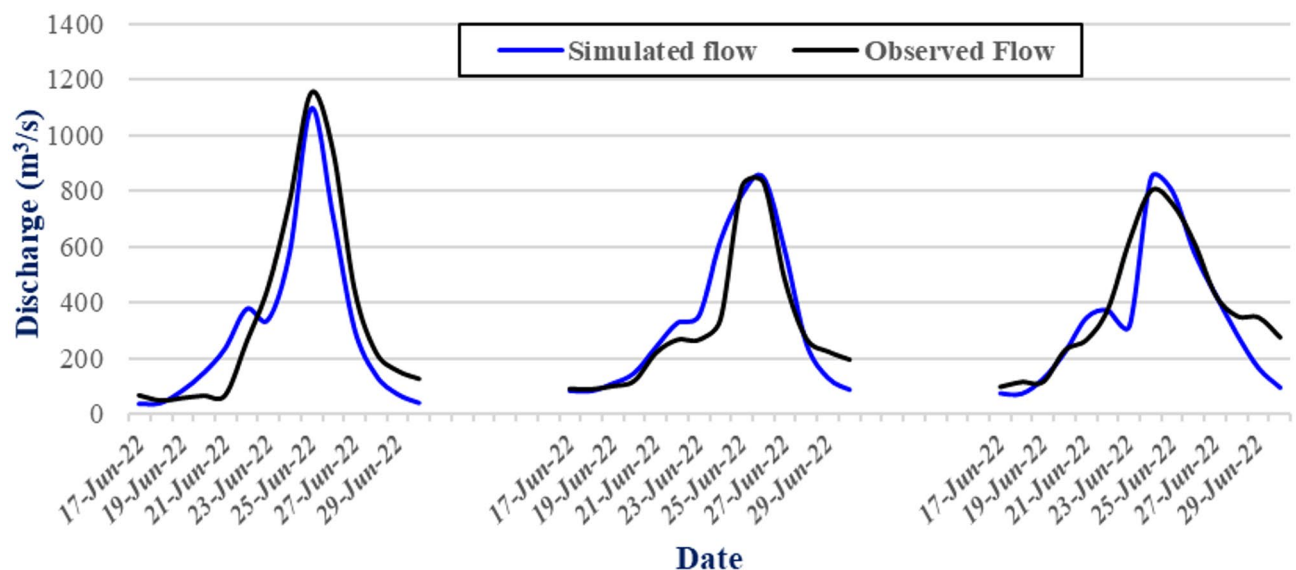
Observed Vs Simulated flow at Sangam, RM Bagh and Asham for Event 3

Fig. 7. Plot of Observed vs. simulated flow at three stations for Event 3 (27-Jul-2021 to 08-Aug-2021).

	Sangam				RM Bagh				Asham			
	R^2	NSE	RSR	PBIAS	R^2	NSE	RSR	PBIAS	R^2	NSE	RSR	PBIAS
Event 1	0.83	0.78	0.50	13.65	0.78	0.70	0.50	9.80	0.79	0.72	0.50	9.13
Event 2	0.93	0.81	0.40	0.97	0.96	0.57	0.60	−20.44	0.92	0.57	0.50	−17.98
Event 3	0.91	0.82	0.40	−14.47	0.98	0.89	0.30	−5.97	0.89	0.76	0.50	−9.09

Table 3. Calibration statistics for storm events at selected Jhelum basin Stations.

Observed Vs Simulated flow at Sangam, RM Bagh and Asham for Event 4

Fig. 8. Plot of Observed vs. simulated flow at three stations for Event 4 (17-June-2022 to 29-June-2022).

assessment and design storm estimation in the study area. The inclusion of spatially distributed soil, land use, and rainfall data likely contributed to this high level of predictive accuracy[89,90].

Design storms for different return periods
The calibrated hydrological model simulated runoff across 24 watersheds of the Jhelum Basin for eight return periods (e.g., 2, 5, 10, 25, 50, 100, 200, 500 years). Results indicate a clear upward trend in design storm intensities

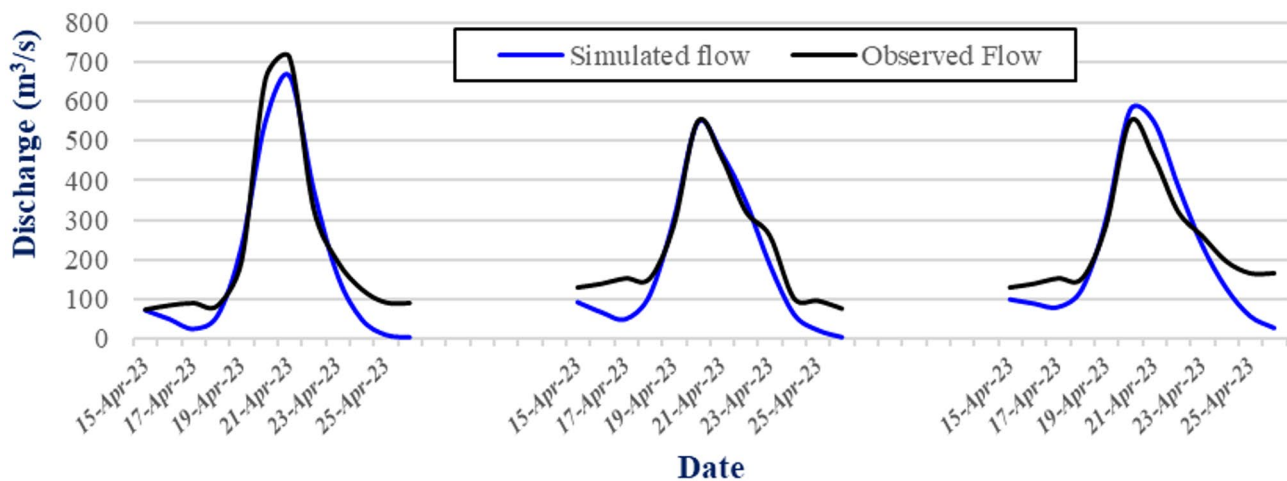**Fig. 9.** Plot of Observed vs. simulated flow at three stations for Event 5 (15-Apr-2023 to 25-Apr-2023).

	Sangam				RM Bagh				Asham			
	R^2	NSE	RSR	PBIAS	R^2	NSE	RSR	PBIAS	R^2	NSE	RSR	PBIAS
Event 4	0.91	0.89	0.30	−13.61	0.88	0.84	0.40	7.35	0.81	0.71	0.50	−12.51
Event 5	0.95	0.92	0.30	−17.68	0.97	0.85	0.40	−17.41	0.94	0.71	0.50	−10.97

Table 4. Validation statistics for storm events at selected Jhelum basin Stations.

(peak discharge in m³/s) with increasing return period (Figs. 10, 11 and 12), reflecting the non-linear escalation of extreme rainfall and runoff responses[91,92]. Table 5 lists peak discharges for each watershed at different return periods, highlighting variability across sub-basins.

Among the watersheds analyzed, upstream watersheds such as Lower Jhelum, Sindh, Lidder and Pohru showed the highest peak discharges at all return periods (Fig. 13), which could be attributed to their larger drainage areas, steep slopes, higher runoff coefficients and orographic precipitation, further supporting their tendency to generate higher peak flows[52,93]. On the contrary, watersheds such as Gundar, Garzan, and Wular II showed lower intensities at all return periods, which could be due to their small catchment areas, larger perviousness or topographic shielding against heavy rainfall events[94]. Surprisingly, watersheds such as Dal, Doodhganga, and Wular I, which are situated in low-lying and comparatively flat regions, reveal moderate to high design storm intensities, particularly over high return periods. This observation is critical, as these watersheds are over the major urban and peri-urban regions of the Kashmir Valley, including Srinagar city and other surrounding settlements, which host dense populations and critical infrastructure[95]. The higher runoff potential witnessed in these basins can be related to larger imperviousness due to urbanisation, land-use changes, and encroachment of natural floodplains[96–98]. Although these urban low-lying areas lack steep slopes, these areas often experience compounded flood risks due to the combined effects of poor drainage, modified hydrological connectivity, and human intervention on natural water bodies[5,99]. The non-linear rise in peak discharge with return period implies that infrastructure designed for moderate events may be increasingly vulnerable under more extreme conditions. This risk is further exacerbated by climate change, which is expected to intensify the hydrological cycle, leading to more frequent and severe rainfall events and accelerating glacier melt[100,101]. The latter may shift flood seasonality in upstream basins, triggering earlier and larger flood peaks beyond the traditional monsoon period.

Due to the data-scarce nature of the Kashmir Valley, particularly in terms of long-term glacier mass balance and snow cover monitoring, the precise influence of changing meltwater regimes on flood return periods remains uncertain and merits further investigation using physically-based models and expanded observational networks[102,103]. These observations highlight the importance of integrated urban flood management and climate-resilient drainage planning in these watersheds.

Statistical spread
The statistical comparison of design storm intensities over return periods (Fig. 14) indicates extreme spatial variability and dispersion increase with growing recurrence intervals[104]. The mean design storms increase from 198.44 mm at the 2-year return period to 1378.25 mm at the 500-year return period, and the increasingly worsening nature of extreme precipitation events in the region is highlighted. The standard deviation also increases from 164.61 mm at the 2-year return period to 1251.01 mm at the 500-year return period, which indicates increasing
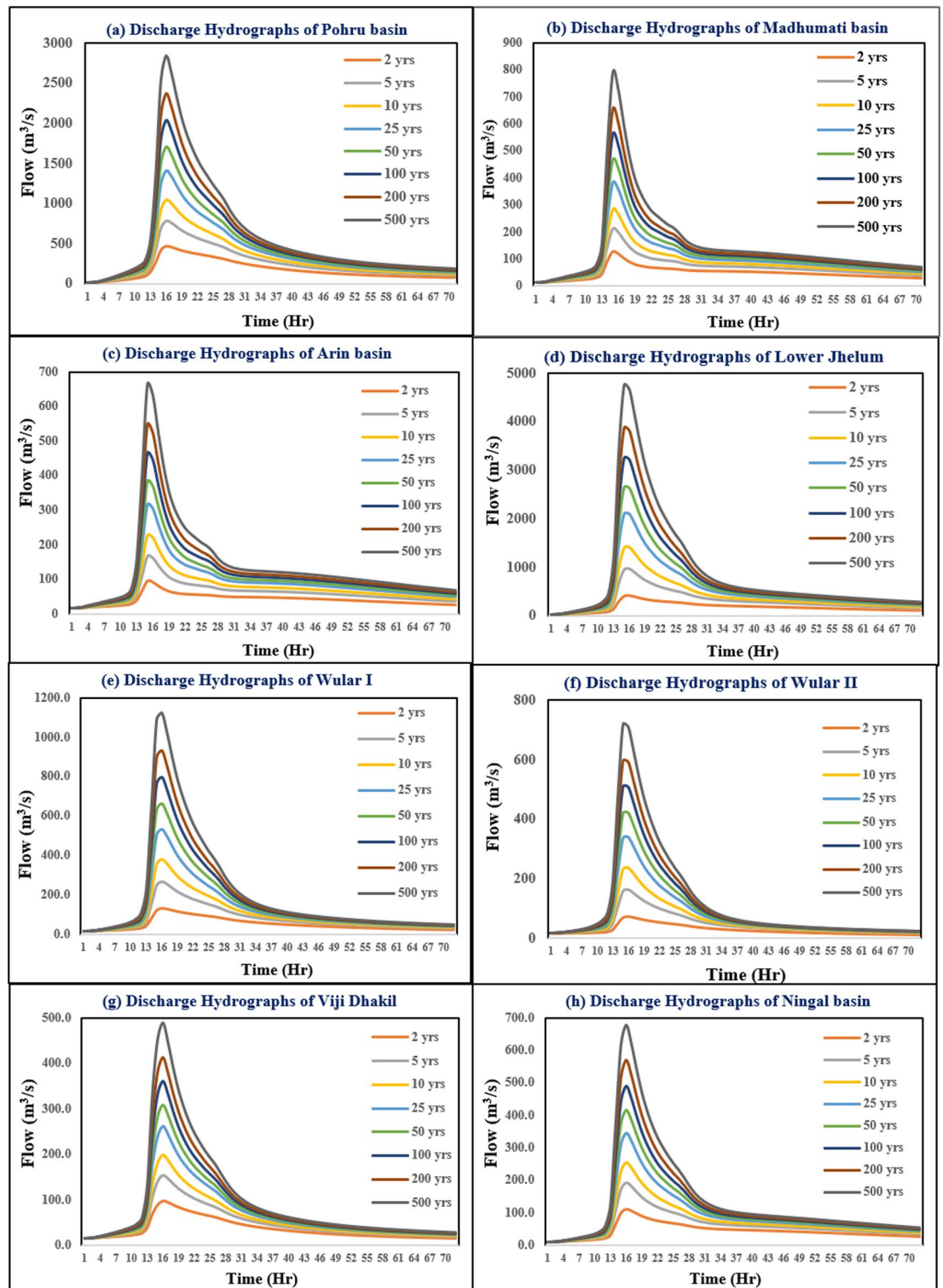
Fig. 10. Design storms at different return periods for the lower subwatersheds of Jhelum basin.

variability in storm intensities among watersheds during rare and extreme events—an event often attributed to different physiographic characteristics, storm tracks, and orographic influences. The interquartile range (IQR), calculated as the difference between Q3 and Q1, also increases with the return period—from 124.26 mm at 2 years to 779.07 mm at 500 years—thus supporting the argument that the behaviour of storms becomes increasingly variable and uncertain under conditions of extreme climate[105]. The maximum design storm at 500-year RP (4750.3 mm in Lower Jhelum) starkly contrasts with the minimum (383.5 mm in Gundar), emphasising the importance of localised flood design and region-specific adaptation strategies, particularly for high-risk
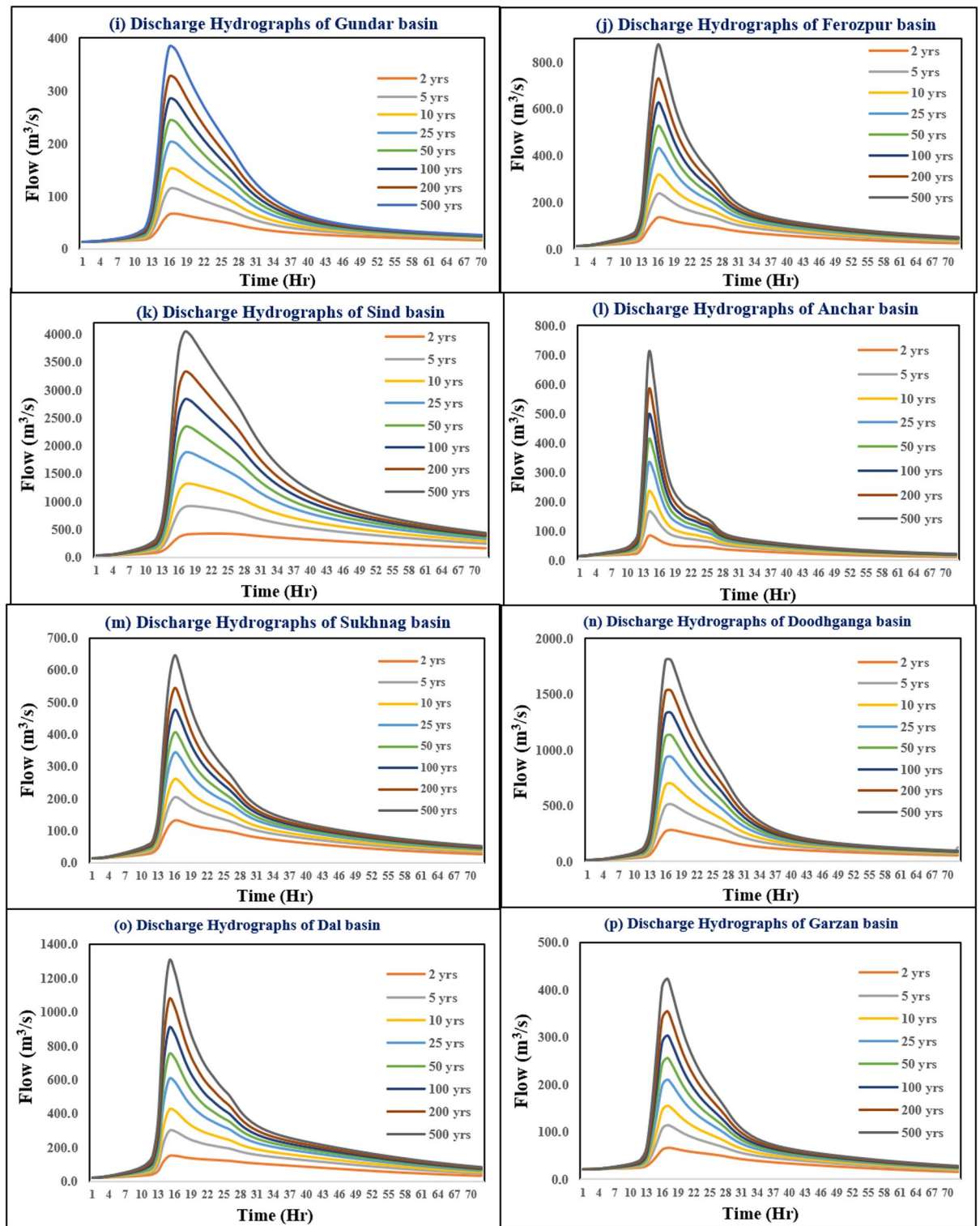
Fig. 11. Design storms at different return periods for the central subwatersheds of Jhelum basin.

watersheds. These findings underscore the necessity of incorporating spatially resolved hydrometeorological data into regional planning to enhance resilience under changing climate regimes.

Recommendations and future scope

The results of this study implies that watersheds such as Lower Jhelum, Lidder and Sindh which show peak discharge from design storms (> 4000 m³/s at 500 return period) require infrastructure designed to withstand such hydrological extremes, which implies that conventional drainage systems, culverts, and bridges often
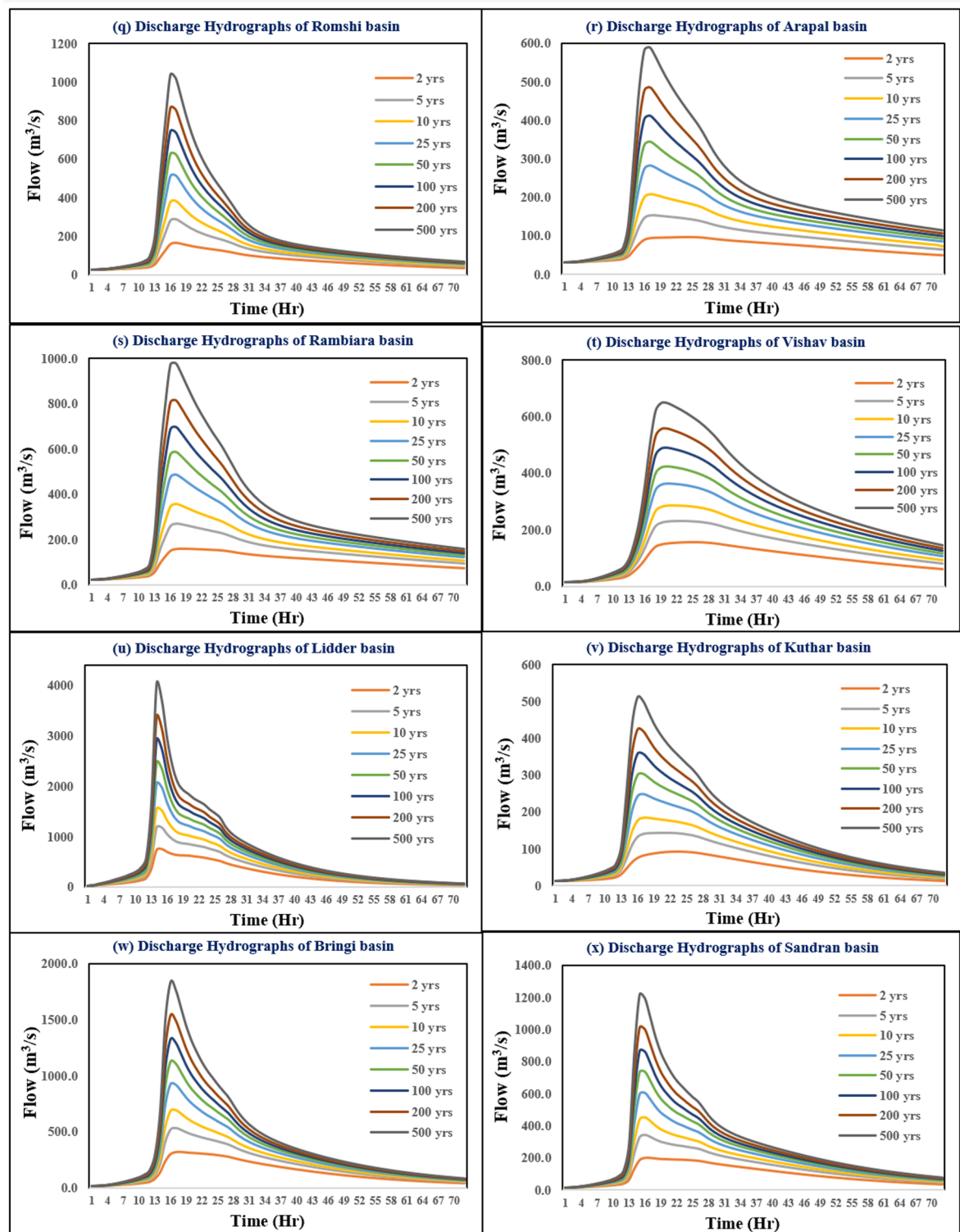
Fig. 12. Design storms at different return periods for the upper subwatersheds of Jhelum basin.

designed for lower thresholds are likely to be overwhelmed, especially in downstream or low-lying areas. Practical adaptation measures include adaptive culvert and bridge sizing based on updated return period analyses, installation of overflow or retention basins in urban areas, and implementation of threshold-based flood alert systems to enable timely evacuations. In urban areas like Doodhganga and Dal which show moderate to high peak discharge from design storms, integrating effective drainage systems with land use planning is essential to mitigate flood risks. The observed increase in variability at higher return periods indicates a growing threat from climate change, highlighting the necessity for comprehensive modelling and adaptive planning. To

S.No	Name of Watershed	2 Year Return period	5 Year Return period	10 Year Return period	25 Year Return period	50 Year Return period	100 Year Return period	200 Year Return period	500 Year Return period
1	Pohru	459.8	777.1	1042.5	1400.4	1703.8	2033.2	2365.0	2843.2
2	Madhumati	126.5	211.8	284.5	383.7	468.8	561.9	655.7	792.2
3	Arin	96.0	168.3	227.0	315.3	385.6	464.2	547.1	664.6
4	Lower Jhelum	403.6	954.9	1416.3	2093.4	2649.8	3243.0	3864.7	4750.3
5	Wular I	128.8	266.6	377.9	533.2	661.8	796.6	932.3	1122.3
6	Wular II	71.1	163.2	237.5	341.1	421.9	508.7	597.2	719.9
7	Viji Dhakil	96.8	154.3	197.9	260.9	308.3	360.0	413.5	488.0
8	Ningal	110.1	192.0	254.3	344.1	415.4	491.5	569.8	678.6
9	Gundar	66.1	115.3	151.9	202.3	242.4	283.8	325.5	383.5
10	Ferozpur	134.1	236.6	317.9	431.3	525.5	624.0	726.8	871.3
11	Sindh	428.3	913.7	1310.6	1882.5	2333.5	2815.5	3316.2	4028.0
12	Anchar	82.4	164.4	232.6	329.5	408.2	492.3	578.2	702.0
13	Sukhnag	130.9	203.0	261.5	342.0	406.4	474.6	544.8	646.1
14	Doodhganga	281.7	518.8	699.9	940.9	1135.4	1333.1	1537.0	1810.6
15	Dal	148.4	297.3	421.5	601.1	747.4	904.5	1070.7	1298.4
16	Garzan	66.2	114.5	154.8	210.7	256.4	303.1	354.2	422.5
17	Romshi	165.3	287.5	384.3	516.2	628.6	746.9	866.0	1038.4
18	Arapal	96.7	153.7	207.1	281.8	345.0	412.0	484.9	589.7
19	Rambiara	158.8	268.8	356.1	487.1	587.1	697.6	814.5	979.1
20	Vishaw	156.3	229.4	285.9	363.2	423.4	490.3	557.3	647.8
21	Lidder	745.2	1187.3	1551.6	2067.0	2474.2	2923.8	3391.2	4036.4
22	Kuthar	93.2	142.9	183.6	249.1	303.5	358.0	423.9	512.3
23	Bringi	315.8	530.6	690.2	927.1	1125.6	1325.4	1537.1	1832.9
24	Sandran	200.5	342.8	449.9	605.8	734.0	869.4	1014.8	1219.9

Table 5. Peak magnitude of design storm in m^3/s for different return periods for 24 Watersheds.
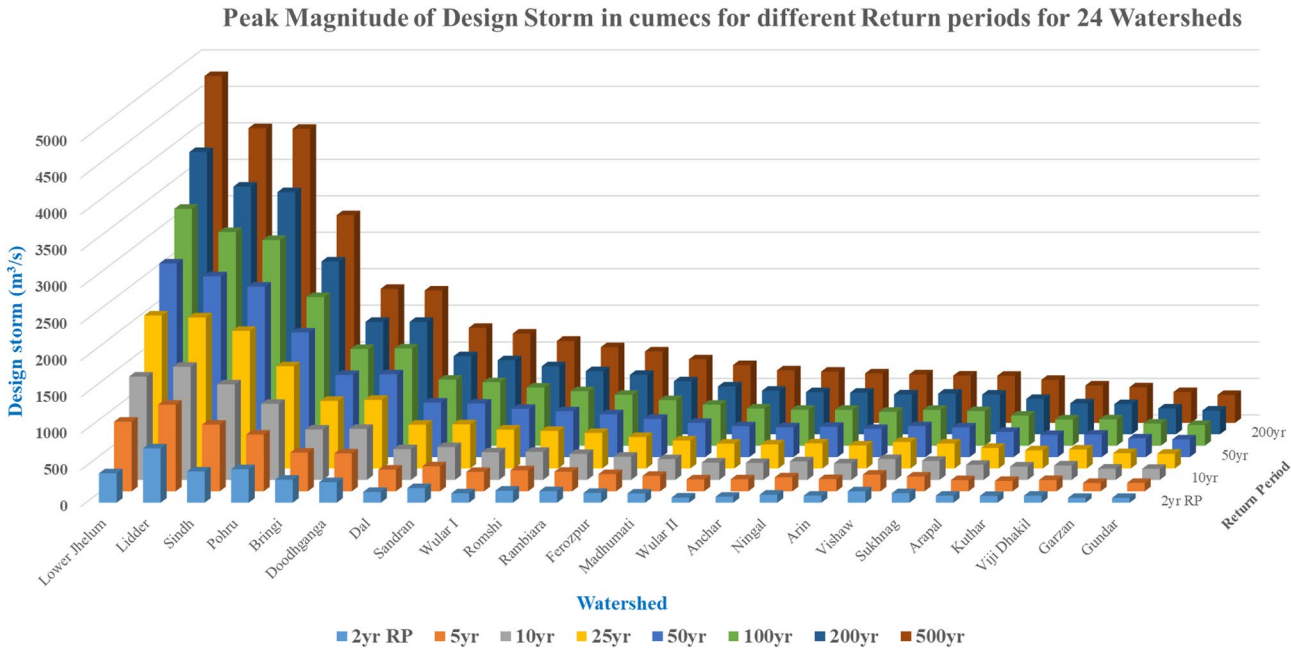

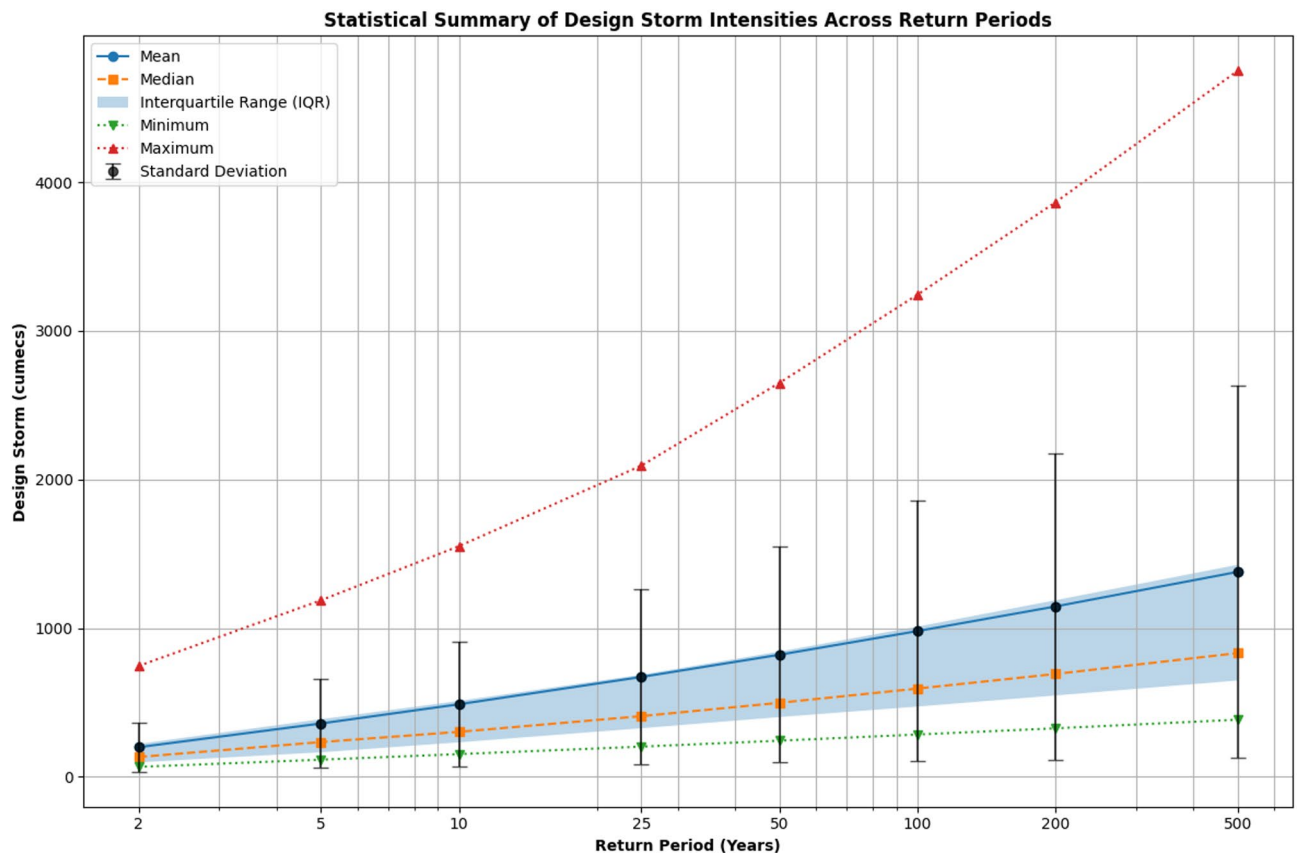**Fig. 13**. Peak magnitude design storm for 24 watersheds.

Fig. 14. Design storms Statistics across Return Periods.

enhance emergency preparedness, authorities should prioritise the installation of automated rainfall gauging systems in high-risk watersheds to validate model data and improve flood forecasting accuracy. Conducting climate resilience assessments using the design storm data can inform watershed development and disaster mitigation programs. Additionally, involving local communities in participatory watershed management will strengthen flood preparedness and facilitate effective dissemination of early warning information.

Due to limited existing studies in the region, the plausibility of design storms at the sub-watershed level could not be validated directly. However, a comparative analysis with regional IDF curves (e.g., from IMD or CWC) is recommended in future work to assess their representativeness and improve reliability for engineering applications. Furthermore, the current study did not extend into flood inundation mapping or infrastructure stress testing; however, this forms a vital scope for future research. The design storms derived herein can serve as critical boundary conditions for flood modelling in HEC-RAS to simulate inundation extents at the sub-watershed level. Such applications will be instrumental in infrastructure vulnerability assessment, optimising dam and reservoir operations, and establishing early warning systems tailored to specific return period scenarios.

Conclusion

This study presents a novel application of HEC-HMS with GIS-based spatial data and gridded satellite rainfall inputs for high-resolution, event-based storm modeling at the sub-watershed scale in the Jhelum Basin, offering a valuable tool for flood risk assessment. The model's strong performance in calibration and validation phases highlights its reliability for hydrological studies in this region. Design storm simulations revealed significant spatial variability in peak discharges across the 24 sub-watersheds. Notably, high-altitude watersheds with larger catchment areas, such as Lower Jhelum, Sindh, Lidder, and Pohru, exhibited higher peak discharges, likely due to their larger drainage areas and steeper slopes. Conversely, urbanized and low-lying areas like Dal, Doodhganga, and Wular I also showed moderate to high peak discharges, underscoring the compounded flood risks from urbanization and reduced infiltration. These findings underscore the necessity for targeted flood mitigation strategies that consider both natural watershed characteristics and anthropogenic influences. Integrating detailed soil, land use, and rainfall data into hydrological models enhances the accuracy of flood predictions and supports the development of effective, region-specific flood management plans. To enhance forecasting accuracy and flood preparedness, agencies are encouraged to install additional rain gauges in data-scarce sub-watersheds of the Jhelum basin, and to integrate real-time hydrometeorological monitoring systems in urban flood-prone zones like Doodhganga and Dal. Sharing basin-scale hydrologic data through open-access repositories would facilitate reproducibility, support policy decisions, and promote collaborative research. Moreover, replicating this modeling framework in other data-scarce Himalayan basins would help develop basin-wide, climate-resilient

flood preparedness strategies. Strengthening data infrastructure and continuously updating land use inputs will further improve the utility of such models for early warning systems and adaptive flood management planning.

Data availability

References

1. Altaf, Y., Ahangar, M. A. & Fahimuddin, M. Water balance study of a high altitude catchment in indus basin of himalayas: application of physics-based distributed hydrologic model-MIKE SHE. *Int. J. Hydrol. Sci. Technol.* **9** (5), 526–549. https://doi.org/10.1504/IJHST.2019.102914 (2019).
2. Grigg, N. S. Comprehensive flood risk assessment: state of the practice. *Hydrology* **10** (2), 46. https://doi.org/10.3390/hydrology10020046 (2023).
3. Marshall, S. R., Tran, T. N. D., Tapas, M. R. & Nguyen, B. Q. Integrating artificial intelligence and machine learning in hydrological modeling for sustainable resource management. *Int. J. River Basin Manag.* 1–17. https://doi.org/10.1080/15715124.2025.2478280 (2025).
4. Pandi, D., Kothandaraman, S. & Kuppusamy, M. Hydrological models: a review. *Int. J. Hydrol. Sci. Technol.* **12** (13), 223–242. https://doi.org/10.1504/IJHST.2021.117540 (2021).
5. Alshammari, E., Rahman, A. A., Ranis, R., Seri, N. A. & Ahmad, F. Investigation of runoff and flooding in urban areas based on hydrology models: A literature review. *Int. J. Geoinf.* **20** (1), 99–119. https://doi.org/10.52939/ijg.v20i1.3033 (2024).
6. Pereira, D. R., Oliveira, A. R., Costa, M. S., Rollnic, M. & Neves, R. Simulation of tidal oscillations in the Pará river estuary using the MOHID-Land hydrological model. *Water* **17** (7), 1048. https://doi.org/10.3390/w17071048 (2025).
7. Sahu, M. K., Shwetha, H. R. & Dwarakish, G. S. State-of-the-art hydrological models and application of the HEC-HMS model: a review. *Model. Earth Syst. Environ.* **9** (3), 3029–3051. https://doi.org/10.1007/s40808-023-01704-7 (2023).
8. Guduru, J. U., Jilo, N. B., Rabba, Z. A. & Namara, W. G. Rainfall-runoff modeling using HEC-HMS model for Meki river watershed, rift Valley basin, Ethiopia. *J. Afr. Earth Sci.* **197**, 104743. https://doi.org/10.1016/j.jafrearsci.2022.104743 (2023).
9. Odey, G. & Cho, Y. Event-based vs. continuous hydrological modeling with HEC-HMS: A review of use cases, methodologies, and performance metrics. *Hydrology* **12** (2), 39. https://doi.org/10.3390/hydrology12020039 (2025).
10. Akhtar, F., Awan, U. K., Borgemeister, C. & Tischbein, B. Coupling remote sensing and hydrological model for evaluating the impacts of climate change on streamflow in data-scarce environment. *Sustainability* **13** (24), 14025. https://doi.org/10.3390/su132414025 (2021).
11. Adnan, R. M., Petroselli, A., Heddam, S., Santos, C. A. G. & Kisi, O. Short term rainfall-runoff modelling using several machine learning methods and a conceptual event-based model. *Stoch. Environ. Res. Risk Assess.* **35** (3), 597–616. https://doi.org/10.1007/s00477-020-01910-0 (2021).
12. Kemp, D. & Alankarage, G. H. Benchmarking three event-based rainfall-runoff routing models on Australian catchments. *Hydrology* **10** (6), 131. https://doi.org/10.3390/hydrology10060131 (2023).
13. Dutta, P. & Sarma, A. K. Hydrological modeling as a tool for water resources management of the data-scarce Brahmaputra basin. *J. Water Clim. Change.* **12** (1), 152–165. https://doi.org/10.2166/wcc.2020.186 (2021).
14. Maidment, D. R. *Handbook of Hydrology*. (McGraw-Hill Inc., New York, 1993). ISBN: 978-0-07-039732-3
15. Hamdan, A. N. A., Almuktar, S. & Scholz, M. Rainfall-runoff modeling using the HEC-HMS model for the Al-Adhaim river catchment, Northern Iraq. *Hydrology* **8** (2), 58. https://doi.org/10.3390/hydrology8020058 (2021).
16. US Army Corps of Engineers Hydrologic Engineering Centre (USACE) & Davis, C. A. *Hydrologic Modeling System: Technical Reference Manual* p. 148 (USACE-HEC, 2000). https://www.hec.usace.army.mil/software/hec-hms/documentation/HEC-HMS_Technical%20Reference%20Manual_(CPD-74B).pdf
17. Natarajan, S. & Radhakrishnan, N. Simulation of rainfall–runoff process for an ungauged catchment using an event-based hydrologic model: A case study of Koraiyar basin in Tiruchirappalli city, India. *J. Earth Syst. Sci.* **130**, 1–19. https://doi.org/10.1007/s12040-020-01532-8 (2021).
18. Kulkarni, A. & Kale, G. Identifying best combination of methodologies for event-based hydrological modeling using HEC-HMS software: a case study on the Panchganga river basin, India. *Sustain. Water Resour. Manag.* **8** (4), 123. https://doi.org/10.1007/s40899-022-00691-4 (2022).
19. Chu, X. & Steinman, A. Event and continuous hydrologic modeling with HEC-HMS. *J. Irrig. Drain. Eng.* **135** (1), 119–124. https://doi.org/10.1061/(ASCE)0733-9437(2009)135:1(119) (2009).
20. Oleyiblo, J. O. & Li, Z. J. Application of HEC-HMS for flood forecasting in Misai and wan'an catchments in China. *Water Sci. Eng.* **3** (1), 14–22. https://doi.org/10.3882/j.issn.1674-2370.2010.01.002 (2010).
21. De Silva, M. M., Weerakoon, S. B. & Herath, S. Modeling of event and continuous flow hydrographs with HEC–HMS: case study in the Kelani river basin, Sri Lanka. *J. Hydrol. Eng.* **19** (4), 800–806. https://doi.org/10.1061/(ASCE)HE.1943-5584.0000846 (2014).
22. Bai, Y., Zhang, Z. & Zhao, W. Assessing the impact of climate change on flood events using HEC-HMS and CMIP5. *Water Air Soil. Pollut.* **230** (6), 119. https://doi.org/10.1007/s11270-019-4159-0 (2019).
23. Azizi, S., Ilderomi, A. R. & Noori, H. Investigating the effects of land use change on flood hydrograph using HEC-HMS hydrologic model (case study: Ekbatan Dam). *Nat. Hazards.* **109** (1), 145–160. https://doi.org/10.1007/s11069-021-04830-6 (2021).
24. Ramly, S. et al. Flood Estimation for SMART control operation using integrated radar rainfall input with the HEC-HMS model. *Water Resour. Manag.* **34**, 3113–3127. https://doi.org/10.1007/s11269-020-02595-4 (2020).
25. Peker, İ. B., Gülbaz, S., Demir, V., Orhan, O. & Beden, N. Integration of HEC-RAS and HEC-HMS with GIS in flood modeling and flood hazard mapping. *Sustainability* **16** (3), 1226. https://doi.org/10.3390/su16031226 (2024).
26. Tangam, S. et al. Daily simulation of the rainfall–runoff relationship in the Sirba river basin in West africa: insights from the HEC-HMS model. *Hydrology* **11** (3), 34. https://doi.org/10.3390/hydrology1103003 (2024).
27. Mandal, S. P. & Chakrabarty, A. Flash flood risk assessment for upper Teesta river basin: using the hydrological modeling system (HEC-HMS) software. *Model. Earth Syst. Environ.* **2**, 1–10. https://doi.org/10.1007/s40808-016-0110-1 (2016).
28. Koneti, S., Sunkara, S. L. & Roy, P. S. Hydrological modeling with respect to impact of land-use and land-cover change on the runoff dynamics in Godavari river basin using the HEC-HMS model. *ISPRS Int. J. Geo-Inf.* **7** (6), 206. https://doi.org/10.3390/ijgi7060206 (2018).

29. Rangari, V. A., Sridhar, V., Umamahesh, N. V. & Patel, A. K. Rainfall runoff modelling of urban area using HEC-HMS: A case study of Hyderabad City. In *Advances in Water Resources Engineering and Management* Vol. 39 (eds AlKhaddar, R. et al.) (Springer, 2020). https://doi.org/10.1007/978-981-13-8181-2_9.

30. Dimri, T., Ahmad, S. & Sharif, M. Hydrological modelling of bhagirathi river basin using HEC-HMS. *J. Appl. Water Eng. Res.* **11** (2), 249–261. https://doi.org/10.1080/23249676.2022.2099471 (2022).

31. Vegad, U., Pokhrel, Y. & Mishra, V. Flood risk assessment for Indian sub-continental river basins. *Hydrol. Earth Syst. Sci.* **28**, 1107–1126. https://doi.org/10.5194/hess-28-1107-2024 (2024).

32. Prakash, C., Ahirwar, A., Lohani, A. K. & Singh, H. P. Comparative analysis of HEC-HMS and SWAT hydrological models for simulating the streamflow in sub-humid tropical region in India. *Environ. Sci. Pollut Res.* **31** (28), 41182–41196. https://doi.org/10.1007/s11356-024-33861-2 (2024).

33. Tibangayuka, N., Mulungu, D. M. & Izdori, F. Evaluating the performance of HBV, HEC-HMS and ANN models in simulating streamflow for a data scarce high-humid tropical catchment in Tanzania. *Hydrol. Sci. J.* **67** (14), 2191–2204. https://doi.org/10.1080/02626667.2022.2137417 (2022).

34. Vo, N. D. et al. Comparing model effectiveness on simulating catchment hydrological regime. In *Advances in Hydroinformatics* (eds Gourbesville, P. et al.) 401–418 (Springer, 2018). https://doi.org/10.1007/978-981-10-7218-5.

35. Mugume, S. N. et al. Development and application of a hybrid artificial neural network model for simulating future stream flows in catchments with limited in situ observed data. *J. Hydroinformatics.* **26** (8), 1944–1969. https://doi.org/10.2166/hydro.2024.066 (2024).

36. Narayana Reddy, B. S. & Pramada, S. K. A hybrid artificial intelligence and semi-distributed model for runoff prediction. *Water Supply.* **22** (7), 6181–6194. https://doi.org/10.2166/ws.2022.239 (2022).

37. Ahmad, I., Farooq, R., Ashraf, M., Waseem, M. & Shangguan, D. Improving flood hazard susceptibility assessment by integrating hydrodynamic modeling with remote sensing and ensemble machine learning. *Nat. Hazards.* **121**, 1–30. https://doi.org/10.1007/s11069-025-07109-2 (2025).

38. Ullah, A., Haider, S. & Farooq, R. Sensitivity analysis of a 2D flood inundation model: A case study of Tous dam. *Environ. Earth Sci.* **83**, 213. https://doi.org/10.1007/s12665-024-11500-w (2024).

39. Tariq, M. A. U. R. et al. Development of a hydrodynamic-based flood-risk management tool for assessing redistribution of expected annual damages in a floodplain. *Water* **13**, 3562. https://doi.org/10.3390/w13243562 (2021).

40. Tariq, M. A. U. R. & Farooq, R. Van de giesen, N. A critical review of flood risk management and the selection of suitable measures. *Appl. Sci.* **10**, 8752. https://doi.org/10.3390/app10238752 (2020).

41. Hanif, F., Kanae, S., Farooq, R., Iqbal, M. R. & Petroselli, A. Impact of satellite-derived land cover resolution using machine learning and hydrological simulations. *Remote Sens.* **15**, 5338. https://doi.org/10.3390/rs15225338 (2023).

42. Malik, I. H. Anthropogenic causes of recent floods in Kashmir valley: A study of 2014 flood. *SN Soc. Sci.* **2** (8), 162. https://doi.org/10.1007/s43545-022-00463-z (2022).

43. Ahmad, W. S., Jamal, S., Sharma, A. & Malik, I. H. Spatiotemporal analysis of urban expansion in Srinagar city, Kashmir. *Discover Cities.* **1** (1), 8. https://doi.org/10.1007/s44327-024-00009-3 (2024).

44. Attar, M. I. et al. Assessment of shift in GWPZs in Kashmir Valley of Northwestern Himalayas. *Environ. Sustain. Indic.* **24**, 100513. https://doi.org/10.1016/j.indic.2024.100513 (2024).

45. Malik, I. H., Ahmed, R., Ford, J. D., Shakoor, M. S. A. & Wani, S. N. Beyond the banks and deluge: Understanding riverscape, flood vulnerability, and responses in Kashmir. *Nat. Hazards.* **120** (14), 13595–13616. https://doi.org/10.1007/s11069-024-06712-z (2024).

46. Ahmed, R. et al. Assessing the climate change impacts in the Jhelum basin of North-Western Himalayas. *Nat. Environ. Pollut Technol.* **24** (S1), 175–185. https://doi.org/10.46488/NEPT.2024.v24iS1.012 (2025).

47. Bhatt, C. M. et al. Satellite-based assessment of the catastrophic Jhelum floods of September 2014, Jammu & Kashmir, India. *Geomatics Nat. Hazards Risk* **8**(2), 309–327 (2017).

48. Ahmad, T., Pandey, A. C. & Kumar, A. Long-term precipitation monitoring and its linkage with flood scenario in changing climate conditions in Kashmir Valley. *Geocarto Int.* **37** (26), 5497–5522. https://doi.org/10.1080/10106049.2021.1923829 (2022).

49. Meraj, G., Romshoo, S. A., Yousuf, A. R., Altaf, S. & Altaf, F. Assessing the influence of watershed characteristics on the flood vulnerability of Jhelum basin in Kashmir himalaya. *Nat. Hazards.* **77**, 153–175. https://doi.org/10.1007/s11069-015-1605-1 (2015).

50. Altaf, Y., Ahangar, M. & Fahimuddin, M. Modelling snowmelt runoff in lidder river basin using coupled model. *Int. J. River Basin Manag.* **18** (2), 167–175. https://doi.org/10.1080/15715124.2019.1634082 (2020).

51. Altaf, S. & Romshoo, S. A. Flood vulnerability assessment of the upper Jhelum basin using HEC-HMS model. *Geocarto Int.* **37** (26), 14699–14720. https://doi.org/10.1080/10106049.2022.2090617 (2022).

52. Parvaze, S., Jain, M. K. & Allaie, S. P. Integrated hydrologic and hydraulic flood modelling for a scarcely gauged inter-montane basin: a case study of Jhelum Basin in Kashmir Valley. *Sādhanā* **48**, 15. https://doi.org/10.1007/s12046-022-02072-1 (2023).

53. Hassan, K. et al. Quantitative analysis of land use land cover (LULC) changes on the hydrological behavior of the Jhelum river basin: North-West himalayas, Kashmir. *Water Conserv. Sci. Eng.* **9** (2), 78. https://doi.org/10.1007/s41101-024-00311-6 (2024).

54. Dar, A. Q. & Maqbool, H. Rainfall intensity-duration-frequency relationship for different regions of Kashmir Valley (J&K) India. *Int. J. Adv. Res. Sci. Eng.* **5** (1), 113–125 (2016).

55. Romshoo, S. A., Rashid, I., Altaf, S. & Dar, G. H. Jammu and Kashmir state: an overview. *Biodivers. Himalaya: Jammu Kashmir State.* 129–166. https://doi.org/10.1007/978-981-32-9174-4_6 (2020).

56. Attar, M. I., Pandey, Y., Naseer, S. & Bangroo, S. A. Soil erosion modelling using GIS-integrated RUSLE of Urpash watershed in lesser Himalayas. *Arab. J. Geosci.* **17** (3), 104. https://doi.org/10.1007/s12517-024-11893-9 (2024).

57. Rashid, I. et al. Projected climate change impacts on vegetation distribution over Kashmir Himalayas. *Clim. Change.* **132**, 601–613. https://doi.org/10.1007/s10584-015-1456-5 (2015).

58. Zaz, S. N., Romshoo, S. A., Krishnamoorthy, R. T. & Viswanadhapalli, Y. Analyses of temperature and precipitation in the Indian Jammu and Kashmir region for the 1980–2016 period: implications for remote influence and extreme events. *Atmos. Chem. Phys.* **19** (1), 15–37. https://doi.org/10.5194/acp-19-15-2019 (2019).

59. Ahmad, L., Kanth, H., Parvaze, R. & Sheraz Mahdi, S. S. Agro-climatic and agro-ecological zones of India. 99–118. (2017). https://doi.org/10.1007/978-3-319-69185-5_15

60. Shafiq, M. U., Rasool, R., Ahmed, P. & Dimri, A. P. Temperature and precipitation trends in Kashmir valley, North Western Himalayas. *Theor. Appl. Climatol.* **135**, 293–304. https://doi.org/10.1007/s00704-018-2377-9 (2019).

61. Islam, Z. U. & Khan, L. A. K. Trends of winter and spring mean snowfall in Kashmir Valley during the period 1981–2005. *Nat. Changes.* **2**, 1–10 (2015).

62. Tassew, B. G., Belete, M. A. & Miegel, K. Application of HEC-HMS model for flow simulation in the lake Tana basin: the case of Gilgel Abay catchment, upper blue nile basin, Ethiopia. *Hydrology* **6** (1), 21. https://doi.org/10.3390/hydrology6010021 (2019).

63. Castro, C. V. & Maidment, D. R. GIS preprocessing for rapid initialization of HEC-HMS hydrological basin models using web-based data services. *Environ. Model. Softw.* **130**, 104732. https://doi.org/10.1016/j.envsoft.2020.104732 (2020).

64. Wang, J., Kumar Shrestha, N., Aghajani Delavar, M., Worku Meshesha, T. & Bhanja, S. N. Modelling watershed and river basin processes in cold climate regions: A review. *Water* **13** (4), 518. https://doi.org/10.3390/w13040518 (2021).

65. SCS, U. *National engineering handbook, Sect. 4: hydrology.* US Soil Conservation Service, USDA, Washington, DC. (1985).

66. Namara, W. G., Damise, T. A. & Tufa, F. G. Rainfall runoff modeling using HEC-HMS: the case of Awash Bello sub-catchment, upper Awash basin, Ethiopia. *Int. J. Environ.* **9** (1), 68–86. https://doi.org/10.3126/ije.v9i1.27588 (2020).

67. Topçuoğlu, M. E., Karagüzel, R. & Doğan, A. Comparison of the SCS-CN and hydrograph separation method for runoff Estimation in an ungauged basin: the Izmit basin, Turkey. *Int. J. Econ. Environ. Geol.* **12** (4), 22–31. https://doi.org/10.46660/ijeeg.v12i4.70 (2021).

68. Clark, C. O. Storage and the unit hydrograph. *Trans. Am. Soc. Civ. Eng.* **110** (1), 1419–1446. https://doi.org/10.1061/TACEAT.0005800 (1945).

69. Kull, D. W. & Feldman, A. D. Evolution of Clark's unit graph method to spatially distributed runoff. *J. Hydrol. Eng.* **3**(1), 9–19. https://doi.org/10.1061/(ASCE)1084-0699 (1998).

70. Kirpich, Z. P. Time of concentration of small agricultural watersheds. *Civ. Eng.* **10** (6), 362 (1940).

71. Jeng, R. I. & Coon, G. C. True form of instantaneous unit hydrograph of linear reservoirs. *J. Irrig. Drain. Eng.* **129**(1), 11–17. https://doi.org/10.1061/(ASCE)0733-9437 (2003).

72. Mateo-Lázaro, J. et al. New analysis method for continuous Base-Flow and availability of water resources based on parallel linear reservoir models. *Water* **10** (4), 465. https://doi.org/10.3390/w10040465 (2018).

73. Rahman, K. U., Balkhair, K. S., Almazroui, M. & Masood, A. Sub-catchments flow losses computation using Muskingum–Cunge routing method and HEC-HMS GIS based techniques, case study of Wadi Al-Lith, Saudi Arabia. *Model. Earth Syst. Environ.* **3**, 1–9. https://doi.org/10.1007/s40808-017-0268-1 (2017).

74. Salvati, A. et al. A systematic review of muskingum flood routing techniques. *Hydrol. Sci. J.* **69** (6), 810–831. https://doi.org/10.1080/02626667.2024.2324132 (2024).

75. Bharali, B. & Misra, U. K. Numerical approach for channel flood routing in an ungauged basin: a case study in Kulsi river basin, India. *Water Conserv. Sci. Eng.* **7** (4), 389–404 (2022).

76. McCarthy, G. T. The unit hydrograph and flood routing. *Conf North. Atl. Div. US Army Corps Eng.* 608–609 (1938).

77. Yu, Z. et al. Simulating the river-basin response to atmospheric forcing by linking a mesoscale meteorological model and hydrologic model system. *J. Hydrol.* **218** (1–2), 72–91. https://doi.org/10.1016/S0022-1694(99)00022-0 (1999).

78. Goodarzi, M. R., Poorattar, M. J., Vazirian, M. & Talebi, A. Evaluation of a weather forecasting model and HEC-HMS for flood forecasting: case study of Talesh catchment. *Appl. Water Sci.* **14** (2), 34. https://doi.org/10.1007/s13201-023-02079-x (2024).

79. Ma, K., Shen, C., Xu, Z. & He, D. Transfer learning framework for streamflow prediction in large-scale transboundary catchments: sensitivity analysis and applicability in data-scarce basins. *J. Geogr. Sci.* **34** (5), 963–984. https://doi.org/10.1007/s11442-024-2235-x (2024).

80. Suryawanshi, V., Honnasiddaiah, R. & Thuvanismail, N. Large-scale flood forecasting in coastal reservoir with hydrological modeling. *Arab. J. Geosci.* **17** (11), 1–17. https://doi.org/10.1007/s12517-024-12109-w (2024).

81. Kumar, N., Singh, S. K., Srivastava, P. K. & Narsimlu, B. SWAT model calibration and uncertainty analysis for streamflow prediction of the tons river basin, india, using sequential uncertainty fitting (SUFI-2) algorithm. *Model. Earth Syst. Environ.* **3**, 1–13. https://doi.org/10.1007/s40808-017-0306-z (2017).

82. Desai, S., Singh, D. K., Islam, A. & Sarangi, A. Multi-site calibration of hydrological model and assessment of water balance in a semi-arid river basin of India. *Quat Int.* **571**, 136–149. https://doi.org/10.1016/j.quaint.2020.11.032 (2021).

83. Ranjan, S. & Singh, V. HEC-HMS based rainfall-runoff model for Punpun river basin. *Water Pract. Technol.* **17** (5), 986–1001. https://doi.org/10.2166/wpt.2022.033 (2022).

84. Serur, A. B. Performance evaluation of hydrological model in simulating streamflow and water balance analysis: Spatiotemporal calibration and validation in the upper Awash sub-basin in Ethiopia. *Sustain. Water Resour. Manag.* **9** (2), 48. https://doi.org/10.1007/s40899-023-00827-0 (2023).

85. Van Griensven, A. V. et al. A global sensitivity analysis tool for the parameters of multi-variable catchment models. *J. Hydrol.* **324** (1–4), 10–23. https://doi.org/10.1016/j.jhydrol.2005.09.008 (2006).

86. Neitsch, S. L., Williams, J. R., Arnold, J. G. & Kiniry, J. R. *Soil and Water Assessment Tool Theoretical Documentation Version 2009*. Texas Water Resources Institute, College Station. https://swat.tamu.edu/media/99192/swat2009-theory.pdf (2011).

87. Faouzi, E. et al. Sensitivity analysis of CN using SCS-CN approach, rain gauges and TRMM satellite data assessment into HEC-HMS hydrological model in the upper basin of Oum Er rbia, Morocco. *Model. Earth Syst. Environ.* **8** (4), 4707–4729. https://doi.org/10.1007/s40808-022-01404-8 (2022).

88. Refsgaard, J. C. Parameterisation, calibration and validation of distributed hydrological models. *J. Hydrol.* **198**, 69–97. https://doi.org/10.1016/S0022-1694(96)03329-X (1997).

89. van Tiel, M., Stahl, K., Freudiger, D. & Seibert, J. Glacio-hydrological model calibration and evaluation. *Wiley Interdiscip Rev. Water.* **7** (6), e1483. https://doi.org/10.1002/wat2.1483 (2020).

90. Arnold, J. G. et al. SWAT: model use, calibration, and validation. *Trans. ASABE.* **55** (4), 1491–1508. https://doi.org/10.13031/2013.42256 (2012).

91. Nepal, S., Flügel, W. A. & Shrestha, A. B. Upstream-downstream linkages of hydrological processes in the Himalayan region. *Ecol. Process.* **3**, 1–16. https://doi.org/10.1186/s13717-014-0019-4 (2014).

92. Qazi, N. Q., Jain, S. K., Thayyen, R. J., Patil, P. R. & Singh, M. K. Hydrology of the Himalayas. *Himal. Weather Clim. Environ.* 419–450. https://doi.org/10.1007/978-3-030-29684-1_21 (2020).

93. Attar, M. I., Khan, J. N., Altaf, Y., Naseer, S. & Bhat, O. A. Development of satellite data based rainfall IDF curves and hyetographs for flood risk management in the Kashmir Valley. *Nat. Hazards.* 1–25. https://doi.org/10.1007/s11069-025-07205-3 (2025).

94. Nilap, A. R., Rajakumara, H. N., Aldrees, A., Majdi, H. S. & Khan, W. A. Storm water runoff studies in built-up watershed areas using curve number and remote sensing techniques. *Discov Sustain.* **6** (1), 1–22. https://doi.org/10.1007/s43621-025-00828-3 (2025).

95. Ali, N., Bhat, M. S., Alam, A., Shah, B. & Sheikh, H. A. Simulating the future flood events and their impacts on critical infrastructure in srinagar: a Himalayan urban centre. *Nat. Hazards.* 1–34. https://doi.org/10.1007/s11069-025-07129-y (2025).

96. Beshir, A. A. & Song, J. Urbanization and its impact on flood hazard: the case of addis ababa, Ethiopia. *Nat. Hazards.* **109**, 1167–1190. https://doi.org/10.1007/s11069-021-04873-9 (2021).

97. Bibi, T. S. & Kara, K. G. Evaluation of climate change, urbanization, and low-impact development practices on urban flooding. *Heliyon* **9** (1). https://doi.org/10.1016/j.heliyon.2023.e12955 (2023).

98. Hosseinzadeh, S. R. The effects of urbanization on the natural drainage patterns and the increase of urban floods: case study metropolis of Mashhad-Iran. *WIT Trans. Ecol. Environ* **84** (2025).

99. Baig, A., Atif, S. & Tahir, A. Urban development and the loss of natural streams leads to increased flooding. *Discov Cities.* **1** (1), 9. https://doi.org/10.1007/s44327-024-00010-w (2024).

100. Bashir, J. & Romshoo, S. A. Bias-corrected climate change projections over the upper indus basin using a multi-model ensemble. *Environ. Sci. Pollut Res.* **30** (23), 64517–64535. https://doi.org/10.1007/s11356-023-26898-2 (2023).

101. Farooq, M. et al. Assessing future agricultural vulnerability in Kashmir valley: Mid- and Late-Century projections using SSP scenarios. *Sustainability* **16** (17), 7691. https://doi.org/10.3390/su16177691 (2024).

102. Gupta, C., Kulkarni, A. V. & Taloor, A. K. Streamflow modeling and contribution of snow and glacier melt runoff in glacierized upper indus basin. *Environ. Monit. Assess.* **193** (11), 761. https://doi.org/10.1007/s10661-021-09537-6 (2021).

103. Nie, Y. et al. Glacial change and hydrological implications in the himalaya and Karakoram. *Nat. Rev. Earth Environ.* **2** (2), 91–106. https://doi.org/10.1038/s43017-020-00124-w (2021).

104. Zhuang, Q., Liu, S. & Zhou, Z. Spatial heterogeneity analysis of short-duration extreme rainfall events in megacities in China. *Water* **12** (12), 3364. https://doi.org/10.3390/w12123364 (2020).
105. Seneviratne, S. I. et al. Changes in climate extremes and their impacts on the natural physical environment. In *Managing the Risks of Extreme Events and Disasters to Advance Climate Change Adaptation*. 109–230 (Cambridge University Press, 2012). https://doi.org/10.1017/9781009157896.013

Acknowledgements

Author contributions

Mohmmad Idrees Attar: Conceptualisation, Methodology, Investigation, Formal analysis, Visualisation, Software, Writing – original draft, review and editing. Junaid Nazir Khan: Writing – review & editing, Methodology, Supervision. Yasir Altaf: Software, Supervision, Data curation, Validation, Writing – review & editing. Majed Alsubih: Writing – review and editing. Sameena Naseer: Software, Resources, Data curation, Rohitashw Kumar: Supervision, Methodology. Owais Ahmad Bhat: Visualisation, Investigation. Shabir Ahmad Bangroo: Resources, Data curation. M. K. Sharma: Supervision, Project administration.

Funding

Declarations

Competing interests

The authors declare no competing interests.

Ethical approval

The author declares that the manuscript has not been submitted to other journals.

Consent to participate

Not Applicable.

Consent to publish

All the authors agree to publish.

Additional information

Supplementary Information The online version contains supplementary material available at https://doi.org/10.1038/s41598-025-17009-x.

Correspondence and requests for materials should be addressed to M.I.A. or Y.A.

Reprints and permissions information is available at www.nature.com/reprints.

Publisher's note Springer Nature remains neutral with regard to jurisdictional claims in published maps and institutional affiliations.